PCT/GB 99/03417
09/807396

The Patent Office

INVESTOR IN PEOPLE

GB99/3417

The Patent Office
Concept House
Cardiff Road
Newport
South Wales
NP10 8QQ

I, the undersigned, being an officer duly authorised in accordance with Section 74(1) and (4) of the Deregulation & Contracting Out Act 1994, to sign and issue certificates on behalf of the Comptroller-General, hereby certify that annexed hereto is a true copy of the documents as originally filed in connection with the patent application identified therein.

In accordance with the Patents (Companies Re-registration) Rules 1982, if a company named in this certificate and any accompanying documents has re-registered under the Companies Act 1980 with the same name as that with which it was registered immediately before re-registration save for the substitution as, or inclusion as, the last part of the name of the words "public limited company" or their equivalents in Welsh, references to the name of the company in this certificate and any accompanying documents shall be treated as references to the name with which it is so re-registered.

In accordance with the rules, the words "public limited company" may be replaced by p.l.c., plc, P.L.C. or PLC.

Re-registration under the Companies Act does not constitute a new legal entity but merely subjects the company to certain additional company law rules.

PRIORITY DOCUMENT
SUBMITTED OR TRANSMITTED IN COMPLIANCE WITH RULE 17.1(a) OR (b)

Signed

Dated 15 NOV 1999

Patents Form 1/77

Patents Act 1977
(Rule 16)

The Patent Office

THE PATENT OFFICE
02 FEB 1999
RECEIVED BY HAND

1/77

03FEB99 E422503-3 D02697
P01/7700 0.00 - 9902332.7

The Patent Office

Cardiff Road
Newport
Gwent NP9 1RH

Request for grant of a patent

(See the notes on the back of this form. You can also get an explanatory leaflet from the Patent Office to help you fill in this form)

1. Your reference

   PA/GC99

2. Patent application number
   (The Patent Office will fill in this part)

   9902332.7

   2 FEB 1999

3. Full name, address and postcode of the or of each applicant *(underline all surnames)*

   KUI MING CHUI
   8 GILBEY CLOSE
   ICKENHAM
   UXBRIDGE
   MIDDLESEX UB10 8TD

   Patents ADP number *(if you know it)*

   6333546001

   If the applicant is a corporate body, give the country/state of its incorporation

4. Title of the invention

   IMAGING

5. Name of your agent *(if you have one)*

   GRAHAM F COLES

   "Address for service" in the United Kingdom to which all correspondence should be sent *(including the postcode)*

   GRAHAM COLES & CO
   24 SEELEYS ROAD
   BEACONSFIELD
   BUCKINGHAMSHIRE
   HP9 1SZ

   Patents ADP number *(if you know it)*

   4361556001

6. If you are declaring priority from one or more earlier patent applications, give the country and the date of filing of the or of each of these earlier applications and *(if you know it)* the or each application number

Country	Priority application number *(if you know it)*	Date of filing *(day / month / year)*

7. If this application is divided or otherwise derived from an earlier UK application, give the number and the filing date of the earlier application

Number of earlier application	Date of filing *(day / month / year)*

8. Is a statement of inventorship and of right to grant of a patent required in support of this request? *(Answer 'Yes' if:*

   a) any applicant named in part 3 is not an inventor, or
   b) there is an inventor who is not named as an applicant, or
   c) any named applicant is a corporate body.
   See note (d))

   NO

9. Enter the number of sheets for any of the following items you are filing with this form. Do not count copies of the same document

Continuation sheets of this form	
Description	24
Claim(s)	
Abstract	
Drawing(s)	17 + 17

10. If you are also filing any of the following, state how many against each item.

Priority documents	
Translations of priority documents	
Statement of inventorship and right to grant of a patent *(Patents Form 7/77)*	
Request for preliminary examination and search *(Patents Form 9/77)*	
Request for substantive examination *(Patents Form 10/77)*	
Any other documents *(please specify)*	

11. I/We request the grant of a patent on the basis of this application.

Signature [signature] Date 2/02/99

12. Name and daytime telephone number of person to contact in the United Kingdom

GRAHAM F COLES ☎ 01494 677181

Warning

After an application for a patent has been filed, the Comptroller of the Patent Office will consider whether publication or communication of the invention should be prohibited or restricted under Section 22 of the Patents Act 1977. You will be informed if it is necessary to prohibit or restrict your invention in this way. Furthermore, if you live in the United Kingdom, Section 23 of the Patents Act 1977 stops you from applying for a patent abroad without first getting written permission from the Patent Office unless an application has been filed at least 6 weeks beforehand in the United Kingdom for a patent for the same invention and either no direction prohibiting publication or communication has been given, or any such direction has been revoked.

Notes

a) If you need help to fill in this form or you have any questions, please contact the Patent Office on 0645 500505.

b) Write your answers in capital letters using black ink or you may type them.

c) If there is not enough space for all the relevant details on any part of this form, please continue on a separate sheet of paper and write "see continuation sheet" in the relevant part(s). Any continuation sheet should be attached to this form.

d) If you have answered 'Yes' Patents Form 7/77 will need to be filed.

e) Once you have filled in the form you must remember to sign and date it.

f) For details of the fee and ways to pay please contact the Patent Office.

Imaging

This invention relates to imaging and in particular to methods and systems for image enhancement.

Imaging is carried out by transfer from the object domain into the image domain, but owing to limiting factors such as the finite size of the energy source, detector size, sampling frequency, display density, software filter function, and possibly partial-volume effects experienced with some imagers, an infinitely fine delta function in the object domain cannot be faithfully reproduced in the image domain. Instead, a smeared-out image, or point-spread function (PSF), is observed. Similarly, an infinitely sharp edge-response function (ERF) in the object domain becomes a smeared-out ERF in the image domain. When two image ERFs are close to each other, the smeared-out effects run into one another. The deterioration of the spatial resolution is often monitored by the percentage modulation transfer which is given by the ratio, expressed in percentage, of the amplitude of the modulation in the image domain to that of the object domain.

The smearing effect becomes more intense as the adjacent ERFs of discontinuities or contrast profiles get closer to each other (or as the spatial frequency of the modulation becomes higher); and this also causes the loss of profile heights. The modulation transfer function (MTF) is the function of the 'normalised' percentage modulation transfer over the whole range of spatial frequency until the cut-off frequency at which the amplitude of the image modulation transferred becomes zero, or, in practice, when it falls below the noise level and becomes undetectable.

The shape of the overall MTF over the full range of spatial frequency is similar to a roll-off sinc function, and the high contrast profile has a higher cut-off spatial frequency than a low contrast profile. Within the working range before the cut-off spatial frequency, the inherent loss of the spatial resolution (that is, the part that is indicated by the smeared-out effect on the corner edge of the ERF) cannot be restored or partially restored even by re-scanning the image with an ultra high resolution digital scanner system.

It is an object of the present invention to provide a method and system by which the above problem can be overcome at least partially.

According to one aspect of the present invention there is provided a method of image enhancement wherein a de-convolution process is applied to the image-domain results of an object-scan to re-construct therefrom the respective point-spread function (PSF) effective in the object- to image-domain transfer at one or more object-discontinuities, and correlating this re-constructed function with the image-domain results of those one or more discontinuities for image-resolution enhancement as to discontinuity-location in the image domain.

According to another of the aspects of the present invention there is provided an image-enhancement system comprising means for performing a de-convolution process on the image-domain results of an object-scan to re-construct therefrom the respective point-spread function (PSF) effective in the object- to image-domain transfer at one or more object-discontinuities, and means to correlate this re-constructed function with the image-domain results of those one or more discontinuities for image-resolution enhancement as to discontinuity-location in the image domain.

A least-squares running filter may be used for the de-convolution process.

In the method and system of the present invention the optimum edge position corresponding to the discontinuity or sharp-edge position of the object ERF may be pin-pointed from the central point of the full-width half-maximum (FWHM) of the image PSF; the pin-pointing may be to sub-pixel accuracy for the image ERF. The original discontinuity or sharp-edge feature of the ERF may then be restored within the image domain by removing the sub-pixel values from outside the optimum edge position to compensate for those within. It is to be noted that the sub-pixels become pixels, and that the enhancement is equivalent to the performance of an extra high resolution image transfer system.

It may be shown mathematically that the image ERF of an infinitely-sharp edge-response function ERF can be reproduced by convoluting the image PSF with the object ERF. This is illustrated in Figure 1 of the accompanying drawings. There is also illustrated in Figure 1 how the image ERF is used in conjunction with the image PSF to determine the optimum edge position from the full-width half maximum FWHM. The optimum edge position corresponding to the sharp edge position of the object ERF may be pin-pointed to sub-pixel accuracy for the image ERF from the central point of the FWHM.

For one-dimensional cases, the operation in accordance with the invention is relatively simple, as only either the X or the Y profile (that is to say, as indicated below, a line spread function (LSF)) is involved). But for the two-dimensional operations, both the X and Y profiles, and if necessary, the XY diagonal profiles to eliminate any possible streakings in the image, may be

involved. In this case, a proper weighting scheme will be required to re-construct the image.

Once the original sharp-edge feature has been pin-pointed, that feature may be restored within the image domain by removing the sub-pixel values from outside the optimum edge position and utilising them for compensation of those within. This enhancement operation is illustrated in the form of the modulation display of Figure 2 of the accompanying drawings.

The technique of the invention may partially recover the loss of the spatial resolution without the trade-off loss of other properties such as image noise. Furthermore, the enhancement of the spatial resolution in an image, of the invention may lead to enlargement or magnification of a small area or particular region of interest (ROI) without blurring (or step) effects at the profile edge, for example as when the sub-pixels are displayed as pixels at the ROI.

A feasibility study using a theoretical data set and the noisy low-contrast magnetic resonance (MR) images of pig brain and lamb kidney surrounded by water have been successfully carried out. The results are illustrated in Figures 3 to 6 of the accompanying drawings, in which Figure 3 shows results for a theoretical data set, Figures 4 and 5 the results achieved for pig brain, and Figure 6 for lamb kidney. The signal-to-noise figures of the re-created PSF (measured by the main peak height to that of the adjacent peaks) were over 8/1.

Figure 7 of the accompanying drawings is a flow chart illustrative by way of example of the image-enhancement system.

The method and system of the invention are applicable, for example, in medical science, in engineering, in physical science and in the field of instrumentation generally. In the context of medical science the invention is especially applicable to diagnostics and treatment planning, and may be utilised in connection with magnetic resonance (MR) imaging, computer assisted tomography (CT), X-ray radiography, film or print copy or digital form, digital X-ray fluorography, ultra-sound imaging, nuclear medicine, positron emission tomography (PET) and other camera or imaging. In MR, X-ray, and CT it may be used, for example, to pin-point the true boundaries of tumour growth or any other abnormal effects essential for the diagnosis, surgery, and radiation treatment. Moreover, the technique is particularly suitable for use in X- ray digital fluorography, in which small structures under study are highlighted by injection of contrast liquids; the small structures may also be isolated from surrounding interfering effects by using an image subtraction technique. The present high-resolution enhancement technique may be used to improve the image quality further.

Image subtraction coupled with the present resolution-enhancement technique may also be applied, for example, to MR images from two different scan-sequences. Also, the magnification of an image ROI without blurring (or step) effects at the edges of the profile has many uses.

The inherent resolutions of X-ray radiography, ultra-sound imaging, nuclear medicine, and PET scanning are relatively low, and some are used for real-time study. Only the individual still frame or hard-copy images may be re-processed.

In the context of engineering, physical science and the field of instrumentation, the invention is applicable to

one-dimensional imaging as used, for example, in regard to bar-code patterns, the spectrum of DNA analysis, iris patterns of eyes (for example, for identification purposes in commercial banking), finger-print identification, and emission spectroscopy. The invention is also applicable to two-dimensional imaging, for example, in relation to images obtained by satellite or pattern recognition, or from a surveillance camera or during laboratory experimentation. As a general matter, the invention is applicable where there needs to be accurate determination of the edge position in an image versus the true object-edge position, for the purpose, for example, of measurement of the positional displacement between object and image, distortion correction and manufacturing control.

As an example of one of many applications of the present invention, a method and system that uses CT and MR imaging in conjunction with one another, will now be described.

The major contribution to the magnetic-resonance (MR) signal comes from the abundant protons content of water molecules and protein. It is a quantum process at the Larmor frequency according to the magnetic field in use. The 'T1-weighted' and 'T2-weighted' MR signals from protons provide contrast numbers that are relative in scale, whereas in CT, the X-ray absorption is a polychromatic attenuation process affected by the electron densities of all the atoms presented within the X-ray beam. There is no equation to correlate the CT number (or the linear attenuation coefficient, electron density, or tissue density) with the MR-contrast numbers; no direct calibration between the two types of signal is possible. This lack of correlation is confirmed by consideration of bone and air which are at opposite ends of the CT contrast (absolute) scale using water as the

base-line reference, but which are at the same end of the MR-image contrast (relative) scale owing to their common low proton-population.

The lack of correlation between the CT and MR signals acts against their use in combination for imaging purposes, but the present invention provides a method and system by which the advantages of each may be utilised to improve image resolution and contrast information.

In the latter regard, CT provides a high spatial resolution but only in regard to view normal to the transverse slice. Resolution for all re-constructed non-transverse planes is poor owing to the need to use elongate voxels to improve signal-to-noise ratio. Also, the partial-volume effect of using elongate voxels may give rise to detection errors at the thin edge of a contrast profile of a lesion. MR, on the other hand, can give the same high degree of spatial resolution viewed in the normal direction to any image-slice plane, and can also provide isotropic resolution with cubic-voxel volume imaging.

To this end, multiple-slice transverse CT scans are collected across a section of the volume of interest in a patient or other subject. Corresponding multiple-slice transverse MR scans of the same volume are collected correspondingly. The slice thickness of the latter scans may be one half, or smaller, of the thickness of the CT slices, and may be collected two-dimensionally or three-dimensionally. The patient is constrained throughout on a couch that provides landmarks with respect to a coordinate reference arrangement on the couch-top. This is to ensure the reproducibility of anatomical positions and features to the first order accuracy for the corresponding CT and MR scans, and also for the final radiation treatment to be made.

The respective transverse planes of the CT and MR images are processed individually in the method and are matched with one another in a de-convoluted space for the CT and MR images, as later explained. The two sets of de-convoluted maps are then merged together to a second order of accuracy in order that the CT numbers may be transferred over to replace the corresponding MR contrast numbers. Once this has been achieved, non-transverse (or oblique) planes can be obtained from the two-dimensional (2D) MR images or from the re-arrangement of the corresponding voxels of the three-dimensional (3D) volume images; where a 2D-MR is used, a further step of contrast transformation may be required.

In the method, CT multiple-slice transverse (Tr) scans are collected across a section of the volume of interest in a patient. Similarly, corresponding MR multiple-slice transverse scans of one half, or smaller, of the slice thickness of the CT slices are collected across the same volume of interest by 2D-MR sampling or 3D-MR sampling.

The patient is constrained from movement during and between the two scanning processes on a couch-top (the 'universal' couch-top described below with reference to Figures 14 and 15, or the 'alternative universal' couch-top described below with reference to Figures 24 and 25), which also provides landmarks within a coordinate reference arrangement defined in the couch-top. The constraint and landmarking is necessary to ensure that anatomical positioning and features are maintained the same to a first order of accuracy for the CT and MR scans, for diagnostic purposes as well as for the final radiation treatment. The respective transverse planes of CT and MR images are processed individually by using 'boundary' or 'finger-print' matching techniques in a de-convolution space (DCS) for the CT & MR images. In these transverse image planes, in particular, the skin-

contours features along the sides of the patient may be best used for second-order alignment and matching purposes, as they are less affected by patient-movements; see Figure 26. The transitional error, dx, may be readily corrected with respect to the coordinate positions of a rectangular tubing system embedded in the couch-top (for example as described below with reference to Figures 24 and 25). The processed data may then be used for a 'diagnostic and statistics software package' of CT image *versus* MR image for their exactly corresponding transverse slice(s), and an associated 'statistical package' for accurate computation of the 'true' area, and then the 'true' volume, of a lesion or tissue profile or contour.

The two sets of de-convoluted maps may also be merged together to a second order of accuracy in order that the CT numbers may be transferred over to replace the corresponding MR contrast numbers. Once this has been done, non-transverse (or oblique) planes are obtained from the 2D-MR image or from the re-arrangement of the corresponding voxels of the 3D-MR volume; in the 2D-MR case, a further step of contrast transformation is required. The transferred contrast data may then be used in a '3D-radiotherapy treatment planning software package' for an in-plane oblique-image pseudo-3D approach using MR images.

Geometrical distortion in the MR images may be corrected to a certain extent, by a combined spin-echo (SE) and field-echo (FE) scan sequence, with the SE part to correct for the field inhomogeneity in B0, and the FE part to overcome the impurity or non-linear gradients. The geometrical distortion may also be dealt with empirically using a post-process correction based on a set of phantom data relating to a drum phantom. Movement problems may be suppressed by some scan sequences and/or

by gating; for certain parts of the body there is no movement problem for the MR scan.

Once the necessary sets of MR images with transferred CT numbers have been obtained, 3D-RTP may be started using the current 2D-RTP software package. The whole '3D-' space is covered through the use of several 2D planes in an in-plane oblique-image pseudo-3D approach.

The optimum-edge determination software sub-routine of the two-dimensional de-convolution technique (2D-DCS) may be used to help map out the 'true' boundaries of the various tissue profiles of an MR image. When the MR scans are carried out on the alternative universal couch-top described below with reference to Figures 24 and 25, embedded with the five MR solutions identified in Table I below, the set of T1 and T2 relaxation times and the standardized proton density with respect to a $CuSO_4.5H_2O$ solution of T1 = T2 = 200 ms, may be each derived for the various tissue contours from the ratio of two MR signal intensities of two different MR scan sequences. They form the 'identification' set from which the tissue types may be identified.

The results obtained may be used to produce an MR diagnostic and statistics software package. From the identity of the tissue type and through the Bulk Heterogeneity Correction method (described by Richard A, Geise *et al* Radiology, 124:133-141, July, 1977), the normalised electron density may then be assigned to each tissue type. With all the tissue contours accordingly mapped out with their respective electron densities, the radiotherapy treatment planning may be smoothly carried out on any MR image. The actual oblique MR image planning will lead to the eventual software package of '3D-radiotherapy treatment planning' using MR images alone. Before the actual planning is started, any

remaining geometry distortion within an MR image may be empirically and accurately corrected by a DCS sub-routine using the geometry distortion correction data in-stored.

The matching technique is based on a method using de-convolution space (DCS) in combination with a least-squares curve-fitting method. These methods are separately well known in pure mathematics, but not, as in the present method and system, combined to produce de-convolution maps with the least-squares fitting curve used as a running filter. The filter is used to overcome practical difficulties due to noise within the image pixels.

For a mathematical model of the method, consideration is given to a line spread function (LSF) arising in the imaging system from an impulse or δ function; this is represented in Figure 8 of the accompanying drawings.

An example of the way in which the LSF of Figure 8 is convolved with an object step-down function to result in a roll-down edge response function (ERF), and how this through the de-convolution process reproduces the LSF, is illustrated in Figure 9 of the accompanying drawings. As illustrated, the LSF is a one dimensional profile across the edge of a contour with its peak position representing the 50%-level point of the ERF.

Figure 9 and the mathematical expressions set out below, indicate the way in which the LSF can be recovered from the resulting ERF at a contrast edge. For convolution related to points 1 to n of the step function:

at point 1:

$$\sum_{0}^{a} L(x)\,\Delta x = E(x)_1$$

at point 2:

$$\sum_{0}^{a} L(x)\,\Delta x - \sum_{a-1}^{a} L(x)\,\Delta x = E(x)_2$$

at point 3:

$$\sum_{0}^{a} L(x)\,\Delta x - \sum_{a-2}^{a} L(x)\,\Delta x = E(x)_3$$

until at point n:

$$\sum_{0}^{a} L(x)\,\Delta x - \sum_{1}^{a} L(x)\,\Delta x = E(x)_n$$

For de-convolution ie. for the ERF to manifest the LSF:

$$E(x)_1 - E(x)_2 = \sum_{a-1}^{a} L(x)\,\Delta x = L(x)_{(a-1)-a}\,\Delta x$$

$$\{E(x)_1 - E(x)_2\}/\Delta x = L(x)_{(a-1)-a}$$

thus:

$$\{E(x)_2 - E(x)_3\}/\Delta x = L(x)_{(a-2)-(a-1)}$$

leading to

$$\{E(x)_{(n-1)} - E(x)_n\}/\Delta x = L(x)_{(n-1)-n}$$

Thus, the same shape of LSF is recovered by the de-convolution process independently of the sense of the ERF; it does not matter whether a roll-up or a roll-down ERF of a positive or a negative contrast profile, is involved. This is an important property as a positive contrast contour will have roll-up (from low to high) ERFs at both ends whereas a negative contrast contour will have roll-down (from high to low) ERFs at both ends.

In the practical implementation, the LSF is derived from the ERF by de-convolution using a running filter. This enhances the accuracy of the method in overcoming the problem of noise that affects the digitised pixel values of the image. Use is made of a least-squares fitting of a set of data points that advances along the whole length of the function from one point to another.

Assuming that $y = a_0 + a_1x + a_2x^2$ represents the ERF curve a five-point or seven-point fit is used, and the normal equation becomes:

$$\begin{vmatrix} \Sigma 1 & \Sigma x_i & \Sigma x_i^2 \\ \Sigma x_i & \Sigma x_i^2 & \Sigma x_i^3 \\ \Sigma x_i^2 & \Sigma x_i^3 & \Sigma x_i^4 \end{vmatrix} \begin{vmatrix} a0 \\ a1 \\ a2 \end{vmatrix} = \begin{vmatrix} \Sigma y_i \\ \Sigma x_i y_i \\ \Sigma x_i^2 y_i \end{vmatrix}$$

where: i is 1+n, ... 5+n; ... until m-5, ... m
or
i is 1+n, ... 7+n; ... until m-7, ... m
n is 0,1, 2, ... ; and
1, ... m is the span of the ERF profile.

The solution may be derived from either:

$$\begin{vmatrix} a0 \\ a1 \\ a2 \end{vmatrix} = \begin{vmatrix} \Sigma 1 & \Sigma x & \Sigma x^2 \\ \Sigma x & \Sigma x^2 & \Sigma x^3 \\ \Sigma x^2 & \Sigma x^3 & \Sigma x^4 \end{vmatrix}^{-1} \begin{vmatrix} \Sigma y \\ \Sigma xy \\ \Sigma x^2 y \end{vmatrix}$$

or:

$$\frac{a0}{\begin{vmatrix} \Sigma y & \Sigma x & \Sigma x^2 \\ \Sigma xy & \Sigma x^2 & \Sigma x^3 \\ \Sigma x^2 y & \Sigma x^3 & \Sigma x^4 \end{vmatrix}} = \frac{a1}{\begin{vmatrix} \Sigma 1 & \Sigma y & \Sigma x^2 \\ \Sigma x & \Sigma xy & \Sigma x^3 \\ \Sigma x^2 & \Sigma x^2 y & \Sigma x^4 \end{vmatrix}} = \frac{a2}{\begin{vmatrix} \Sigma 1 & \Sigma x & \Sigma y \\ \Sigma x & \Sigma x^2 & \Sigma xy \\ \Sigma x^2 & \Sigma x^3 & \Sigma x^2 y \end{vmatrix}} = \frac{1}{\begin{vmatrix} \Sigma 1 & \Sigma x & \Sigma x^2 \\ \Sigma x & \Sigma x^2 & \Sigma x^3 \\ \Sigma x^2 & \Sigma x^3 & \Sigma x^4 \end{vmatrix}}$$

For both of these equations to be valid:-

$$\begin{vmatrix} \Sigma 1 & \Sigma x & \Sigma x^2 \\ \Sigma x & \Sigma x^2 & \Sigma x^3 \\ \Sigma x^2 & \Sigma x^3 & \Sigma x^4 \end{vmatrix} \neq 0$$

The gradient at $dy/dx_{(3+n)}$ or $dy/dx_{(4+n)}$ can then be derived and plotted against x for the LSF profile.

The graph of dy/dx against x gives the LSF profile. The peak of this profile is located half way between the mid-points of the ascending and descending limbs of the graph and is derived from this as the so-called full-width-half-maximum (FWHM) with an accuracy to the sub-pixel level.

The point spread function (PSF) is the two dimensional profile which may be derived, in practice, from the two corresponding LSFs orthogonal to one another within an image plane. The peak position of the PSF profile is, therefore, from the 'mean' or 'cross-over' of the two peaks or the two LSF profiles. The PSF is obtained in practice from two orthogonal axes in a two-dimensional plane.

The waveform relationships between real space (RS), image space (IS), and de-convolution space (DCS) are illustrated at (a), (b) and (c) respectively of Figure 10 of the accompanying drawings. These show the relationship between peak positions p1, p2, p1', p2',p1" and p2" and dip positions d' and d" in the DCS, with the positions and magnitudes of contrast value of the waveforms in the image space (IS) and real space (RS), and highlight certain useful properties of the process. In particular, the tail-end to tail-end distance of each LSF profile gives a spread of 100% down to 0%, and *vice versa*, in the corresponding ERF profile in IS. Also, the half way points of the full-width-half-maximum (FWHM) in

the LSF profiles give the peak positions of p1, p2, p1', p2', p1", and p2" which correspond to the 50% level points of their related ERF profiles; the dip positions d' and d" in the LSF profiles correspond to the central maxima or minima of the profiles in IS, and the distances of p1' to p2', and p1" to p2" correspond to the FWHMs of the profiles in the IS and the distances between the edges of the step function in RS.

From the above, the generation of the LSF (or PSF) is independent of the roll-up or roll-down nature of ERFs at the edges of the contrast contour. In other words, it is independent of the sense and the absolute value of the contrast numbers within the contour. The peak position of the LSF (or PSF) is the central half-way (50%) point of the roll-up or roll-down ERF which is the optimum position at which the two sets of ERFs are matched together with the overall effect of not distorting the contour shape within the boundary of the ERFs.

In order to match or merge together the two corresponding CT and MR images, they are transformed into DCS. In DCS the peaks of the LSFs (or PSFs) mark the central half-way points of the ERFs of the original two-dimensional image planes. These peak positions are then linked together to form the 'de-convolution' or 'finger-print' maps. Through the assistance of these maps, the two image files may now be matched or merged together to a second order of accuracy. Figures 11 and 12 of the accompanying drawings illustrate one-dimensional and two-dimensional generation of de-convolution or finger-print maps in DCS.

The subsequent transformation of the contrast numbers is guided by a moving sub-set filter conformed by the sub-set mean values and the overall uniformity of the profile of the MR image; this filter is quite similar to the running filter used for the conversion of ERF to LSF.

The number of samples in the moving sub-set filter may also be used for the cut-off rejection of small or 'point' contours, that is to say, spurious contours introduced by noise, within the CT or MR image.

A similar technique is employed for MR(Tr) to MR(Oblique) transformation of contrast numbers. Since a high spatial resolution and small partial volume effect are maintained for the thin 2D-MR(Oblique) slice or the 3D-MR(Oblique) plane, the transformation is relatively simple. Through this DCS technique, the high spatial resolution operation is maintained throughout the whole process of re-processing.

The combined MR and CT method of the invention requires the matching of corresponding CT and MR images with one another, and it is important that the same 'laid-out' features of anatomy are presented for the each scanning activity, and that the same features are presented again for radiation treatment. The couch-top is used for this and the landmarks and reference axes defined in it are encoded into the images, for use as guides for the repositioning of the patient for any subsequent scanning or other activities, and also for the first order alignment in the initial matching of CT and MR images (allowing more refined matching to the second order of accuracy using the DCS technique, to be initiated).

The form of the couch-top used will now be described with reference to Figures 13 to 15 of the accompanying drawings.

Referring to Figure 13 to 15, the couch-top has a flat upper part 100 that is carried by a curved lower part 101 which fits to the scanner table of the CT or MR installation. The patient lies on the flat part 100 and is constrained on it (by an arrangement not shown), so as

to reproduce the same anatomical features for scanning and treatment; the treatment table similarly has a flat surface.

An X-tubing array 102 is embedded into the upper part 100. The tubing of the array 102 is of plastics or glass having an external diameter of up to 6 mm and an internal diameter of up to 3 mm, and is filled with a chemical solution of $MnCl_2$. The cross-sectional image of such tubing will show a positive profile for MR and a negative profile for CT. However, the DCS technique of processing these images pin-points their centres irrespective of the contrast values represented.

As shown in Figure 14, the patient is constrained by the constraint arrangement to lie lengthwise of the flat part 100 (ie along the z-axis of the coordinate system defined in the couch-top) and centrally of it (ie with respect to the lateral x-axis); the patient's head is placed on a head-rest 103 suitable for the scan, CT or MR, to be undertaken. Three landmarkers/constraint levers 104, two under the armpits and one at the crotch between the thighs, are also used to position the patient as well as to provide some form of conformation with respect to the reference coordinate system. Air-compressed cushions (not shown) may be gently pressed in from either sides to conform the limbs and hence the body along its length.

The X-tubing array 102 inside the bottom flat part 100 may be used as the reference system for the transverse and sagittal planes, and the oblique planes between them. The flat surface of the part 100 or the flat contour of the patient's skin surface in contact with it may be used as the datum for the coronal planes. However, an extra small X-tubing array (not shown) may be placed above the patient using the three landmarkers as the supporting legs; this enables the small-angled oblique planes

between the coronal and transverse planes to be monitored.

If the internal-bore diameter of the magnet of the MR scanner is large enough, an extra X-tubing array 105 (Figure 15) may be used along either side of the patient to help in monitoring the small-angled oblique planes between the coronal and sagittal planes. Furthermore, a curved X-tubing array (not shown) may be placed inside and on the bottom of the head rest (or head coil) 103 used for the MR scan for the purpose of clearly establishing the coordinates of the head.

If the internal-bore diameter of the magnet of the MR scanner is not large enough for the extra array 105 to be fitted, then the 'alternative universal couch-top' of Figures 24 and 25 may be used; Figure 25 is a section taken on the line XXV-XXV of Figure 24. As illustrated in Figures 24 and 25, the bottom X-tubing pattern is in this case replaced by tubing 110 having a zig-zag pattern throughout the length of the couch-top. Extra capacity is provided by straight tubing 111 that extends centrally lengthwise of the couch-top.

The tubing 110 of zig-zag pattern may be as illustrated in the detail of Figure 24 and in Figure 25, formed by double-layer tubing of rectangular cross-section, so that edge-position determinations may become one-dimensional when applying the de-convolution space subroutine (i.e. 1D-DCS subroutine); the tubing 111 may of single-layer rectangular cross-section as illustrated. The rectangular tubing 110 and 111 may be filled as indicated in Figure 25 with the five MR solutions S_0 to S_4 of Table I, for standardisation and calibration purposes for applications in the MR 'diagnostic and statistics software package' and the stand-alone MR method for the '3D-radiotherapy treatment planning software package'.

From the five MR solutions S_0 to S_4, choice may be made from the four $MnCl_2.4H_2O$ solutions, S_1 to S_4, to cover the full range of values of T1 and T2 for anatomical tissues, and of the fifth solution, S_0, of $CuSO_4.5H_2O$, that is 'equivalent' to "loosely bound water" (see pages 34-38 of 'NMR, A Primer for Medical Imaging' by G.L. Wolf *et al*, published by Slack Incorporated, 1984).

Examples of solutions S_0 to S_4 are as set out in Table I, as follows:

Table I

Solution		T_1 at 0.5T	T_2 at 0.5T
S_0	1.25 g/l $CuSO_4.5H_2O$	200 ms	200 ms
S_1	$3.41x10^{16}$ Mn^{+2} ions/ml	840 ms	300 ms
S_2	$1.15x10^{17}$ Mn^{+2} ions/ml	440 ms	120 ms
S_3	$2.30x10^{17}$ Mn^{+2} ions/ml	250 ms	60 ms
S_4	$4.37x10^{17}$ Mn^{+2} ions/ml	150 ms	30 ms

Figure 27 shows a form of cover that may be used for suppressing movement of, in particular, the patient's abdomen. The cover is of polystyrene sheet 120 with cushioning 121 around apertures for the patient's legs. The sheet 120 is secured over the patient and between his/her legs using fabric elements 122 that establish with an underlay (not shown) releasable fixings of fabric hook-and-eye form (for example, as sold under the Registered Trade Mark VELCRO).

The material of the couch-top is carbon fibre so as to ensure a low linear attenuation coefficient with transparency to X-rays. Edges of the couch-top are smoothly rounded to avoid sharp edges that would cause

streaking in the CT image. Non-magnetic material is used throughout to avoid disturbing the uniform magnetic field, B0, used for MR.

The radiation treatment table needs to be capable of both translational, "in and out" movement as well as rotational movement to cover the 3D planning and treatment.

A final empirical correction of any residual geometrical distortion may be carried out using a cylindrical or elliptical drum phantom. A cylindrical drum phantom is illustrated in Figures 16 and 17, and an elliptical drum phantom in Figures 18 and 19 of the accompanying drawings.

Referring to Figures 16 and 17, the cylindrical drum phantom, which may be of about 160 mm in length and is for use with the head coil of the scanner, includes a central rod 200 of polymethyl methacrylate (as sold under the Registered Trade Mark PERSPEX) having a diameter of about 2 mm and defining the phantom centre, Cph. The body of the phantom is built up as concentric sections about the rod 200, each comprising evenly-spaced blocks 201 of polymethyl methacrylate and with the blocks 201 of each section in exact register radially with the gaps 202 between the blocks 201 of the preceding section. The central region 203, having a diameter of about 20 mm, may be left blank (since the magnetic field within the central region is uniform to within 0.1 ppm, so no B0 correction is required). The gaps 202 and the central region 203 are filled with an NMR solution (e.g. $MnCl_2$ or $CuSO_4$).

Peak positions of the PSFs in the DCS map for the drum are derived and stored. This data is then corrected for each point of the map with respect to the iso-centre of

the scanner system, Ciso, using the following vector equation:-

$$\Delta r = r_2 - r_1$$

where Δr is the correction vector between Ciso and Cph; and
r_2 and r_1 are the vectors to the relevant point of the map from Ciso and Cph respectively.

The elliptical drum-phantom of Figures 18 and 19 is constructed in essentially the same manner as the cylindrical drum phantom, and is for use with the body coil of the scanner. The major and minor axes are chosen according to the field of view being studied.

As an alternative, the cylindrical and elliptical drum phantoms may be constructed as shown in Figures 20 and 21, using thin plates 300 of polymethyl methacrylate instead of the blocks used for the phantoms of Figures 16 to 19. The plates 300, which may have a thickness of between 1.5 mm and 2.0 mm, are spaced radially from one another by gaps 301 that, together with the central region 302 are filled with appropriate NMR solution.

CT scan images are not subject to geometrical distortion so CT scan data accumulated using the phantoms, and the DCS profile data consequently derived and stored, are used as a datum or reference set for correction of the MR scans. Such corrections also automatically correct for manufacturing tolerances, and the DCS data derived from the phantom through the CT and MR scans represents a reference situation devoid of motion.

The DCS technique described above is applicable further in diagnosis and treatment. In particular, it may be used to assist visual detection of gradual change of

contrast level in scan images. For example, as illustrated in Figure 22 of the accompanying drawings, the 100% point at which the roll-off of a lesion profile begins can be readily plotted from the DCS profile, together with the 50%-level point, and then the 0% point where the profile has completely levelled off. Graphic representations of these various points can then be plotted out to facilitate diagnosis, as illustrated in Figure 23 of the accompanying drawings, in the form of a string of characters 400 delineating the 100%-level, a string of characters 401 delineating the 50%-level and a string of characters 402 delineating the 0% level.

In current radiation treatment planning, a composite volume leaving a margin of 15 mm around a lesion, is used. To be effective, the tail-end of the lesion growth is to be within the treatment-beam path, and in this regard there is advantage in extending the DCS-profile plot of Figure 22 to include a point which is a distance (d) beyond the 0%-level. This is then used for diagnosis and treatment, to establish an outer string of characters 403 in the graphical representation of Figure 23. The distance (d) covers the penumbra-spread as well as any possible mis-alignment by the operator.

The de-convolution space (DCS) technique leads to two major software packages for: (a) optimum edge determinations, and (b) spatial resolution enhancement. Applications that may be derived from these packages are identified in the flow-chart of Figure 28.

From the software for both optimum edge determinations (for image profiles and artificial edges) and spatial resolution enhancement for all one- and two-dimensional images, products for both medical and non-medical applications may be provided as follows:

(1) software package for the spatial resolution enhancement and the enlargement of all two-dimensional image-regions of interest free of smearing (or step) effects at the image-profile edges;

(2) software package for the spatial resolution enhancement and enlargement of all one-dimensional images-regions of interest free of smearing (or step) effects at the image-profile edges;

(3) software package for accurate edge determinations for all one-dimensional and two-dimensional images for multiple applications; and

(4) image-enhancement hardware system to cover the areas of software packages (1)-(3).

From the software for optimum edge determinations (for image profiles and artificial edges) alone, the following hardware and software packages for medical applications may be provided:

(1) a section or full-scale section of the 'alternative universal couch-top' design for first- and second-order alignments and standardisation purposes for applications as identified in items (2) to (6) below;

(2) an empirical geometry-distortion correction package for MR imaging;

(3) a diagnostic and statistics package of 2D(CT) image *versus* 2D(MRI) image of exactly-corresponding transverse slices - the

statistics package may help to compute the accurate area within the 'true' boundaries of a lesion or a tissue profile, and then follow-up with the eventual calculation of the 'true' volume of such profile or effect (other statistical approaches may also be performed within the tissue boundaries - for example, within these boundaries, noise grains may be ironed out if necessary by taking the mean of the output of a long-running filter across the whole profile);

(4) MR diagnostic and statistics package to compute accurately the T1 and T2 relaxation times and the standardized proton density of the tissue profiles for diagnostic purposes, and to perform the same statistics as that of package (3);

(5) a combined CT & MR method using the multiple-slice data of item (3) for three-dimensional radiotherapy treatment planning within the oblique MR image planes; and

(6) a stand-alone MR method using the calculated T1, T2 and the standardised proton density within the tissue profiles of the multiple-slice image-data of item (4) in order to identify the tissue types and then to obtain the electron densities through the Bulk Heterogeneity Correction method so that the three-dimensional radiotherapy treatment planning within the general oblique MR image planes may be carried out.

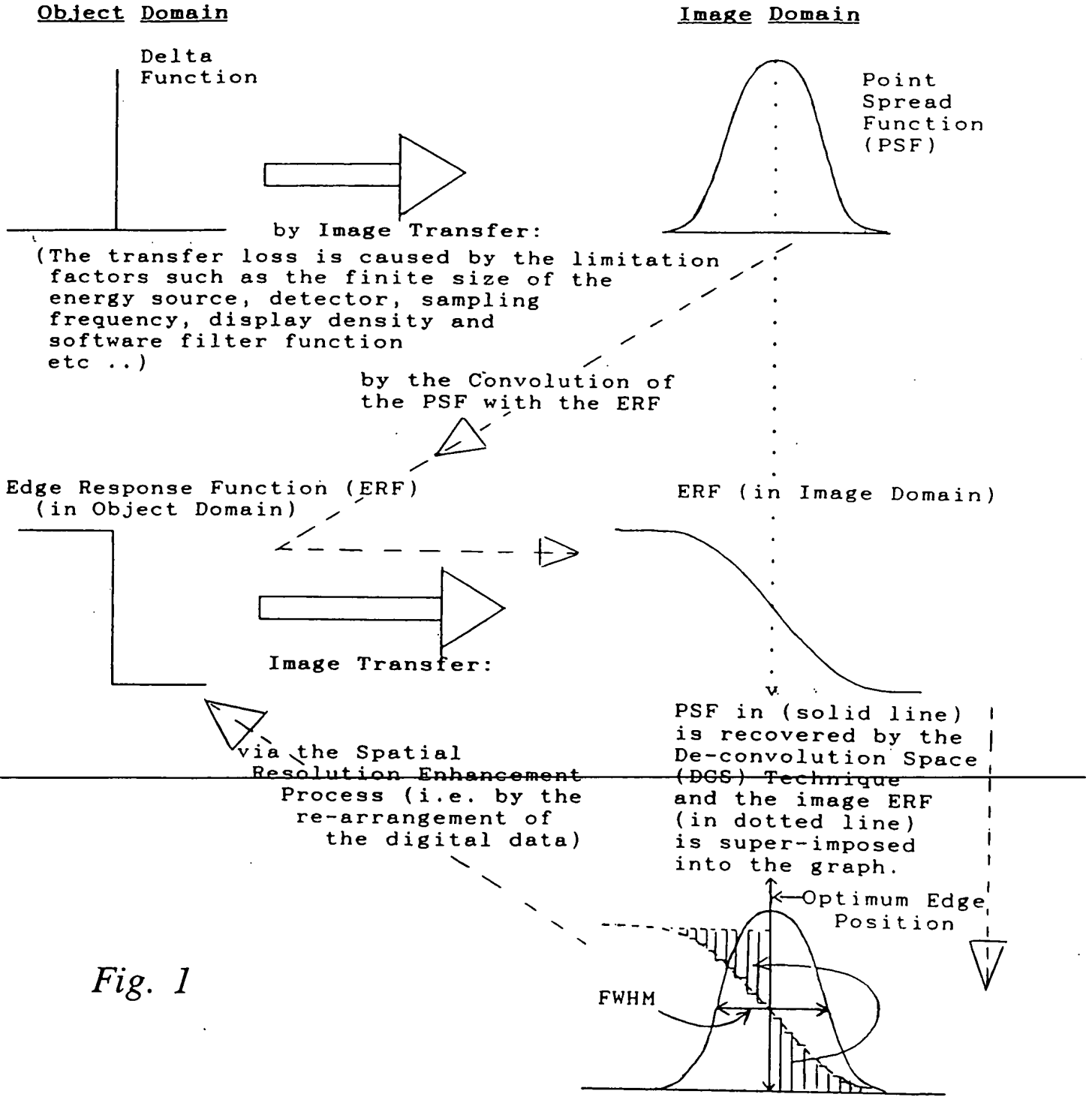
Object Domain
Image Domain
Delta Function
Point Spread Function (PSF)
by Image Transfer:
(The transfer loss is caused by the limitation factors such as the finite size of the energy source, detector, sampling frequency, display density and software filter function etc ..)
by the Convolution of the PSF with the ERF
Edge Response Function (ERF) (in Object Domain)
ERF (in Image Domain)
Image Transfer:
via the Spatial Resolution Enhancement Process (i.e. by the re-arrangement of the digital data)
PSF in (solid line) is recovered by the De-convolution Space (DCS) Technique and the image ERF (in dotted line) is super-imposed into the graph.
Optimum Edge Position
FWHM

Fig. 1

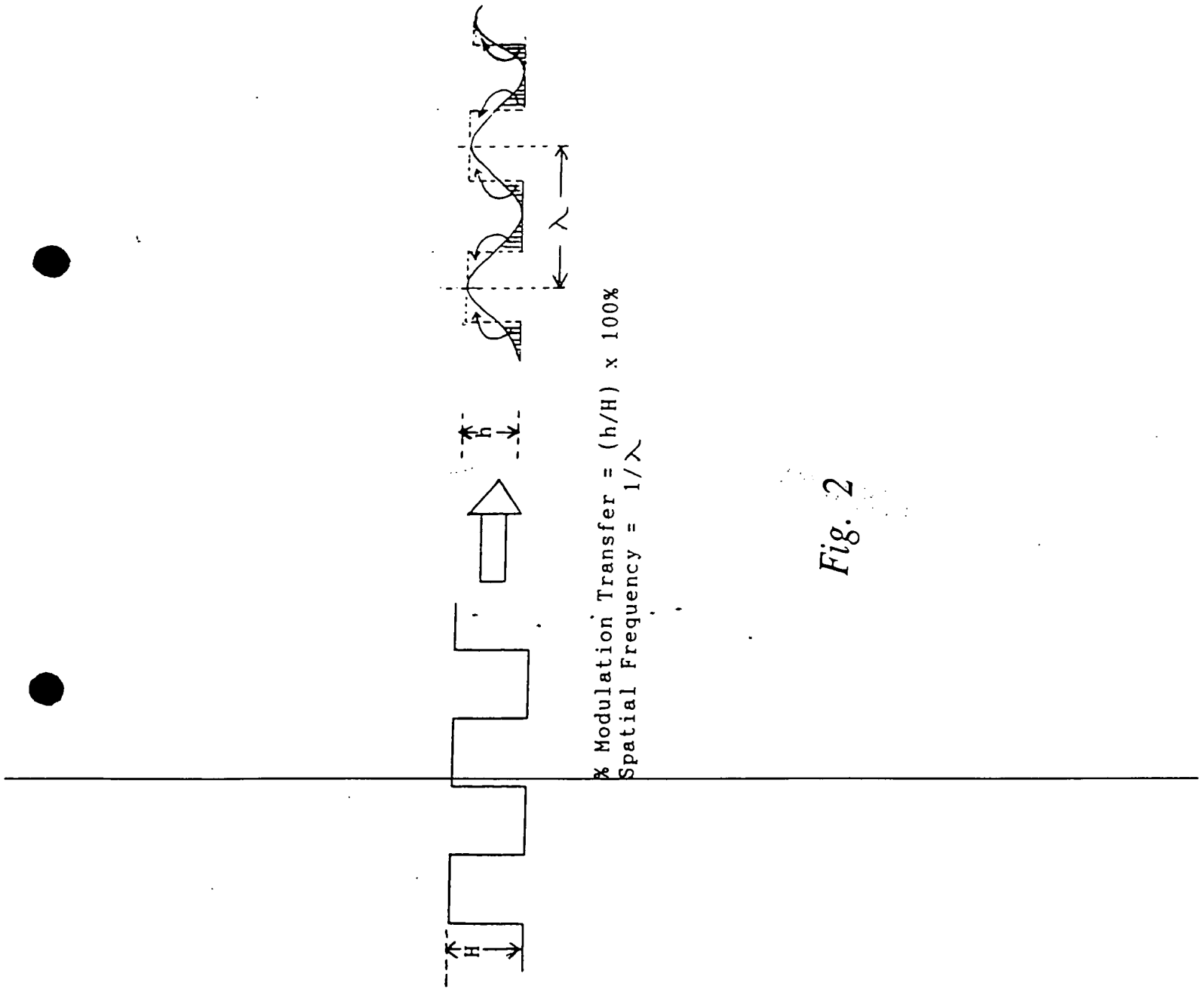

Fig. 2

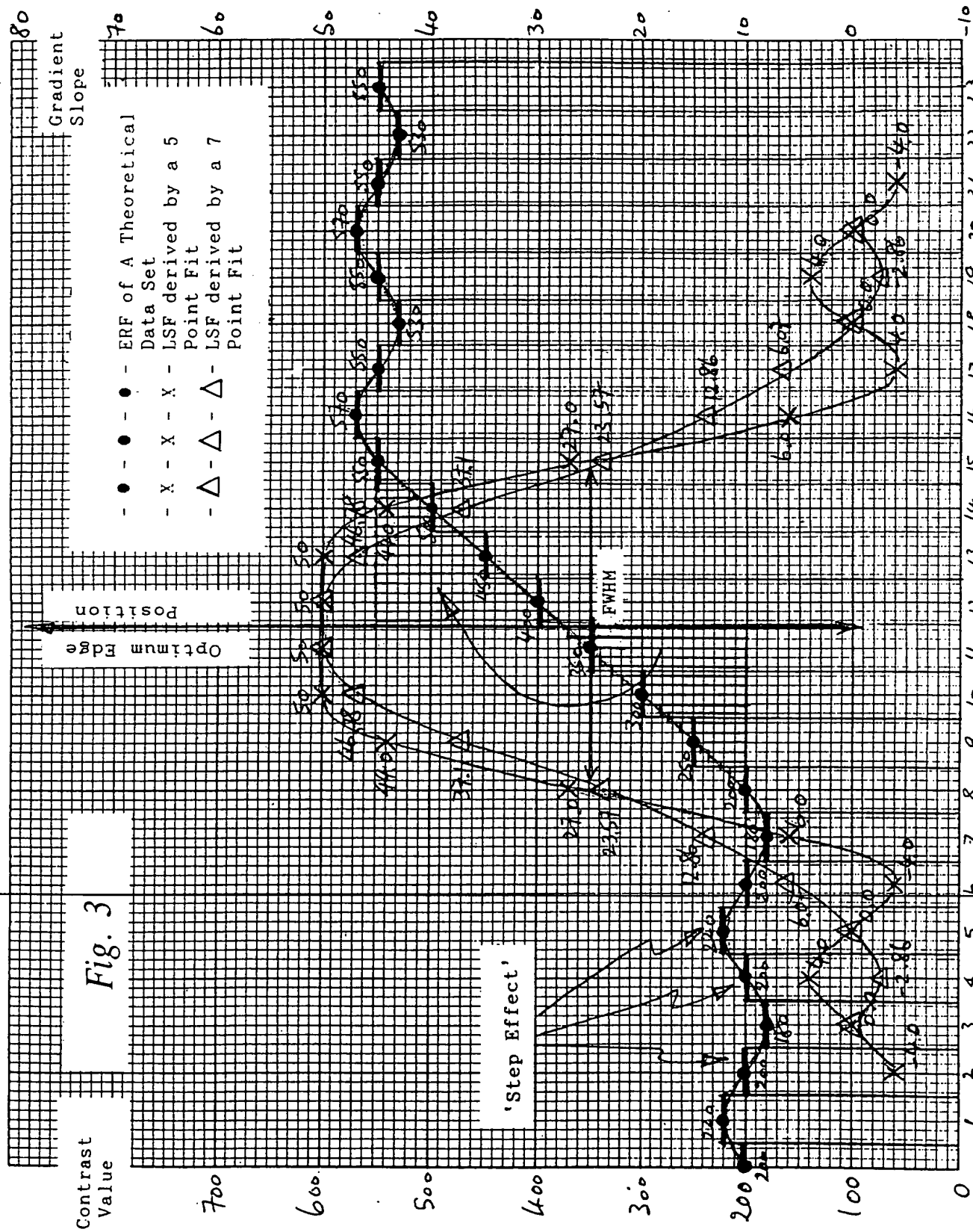
Gradient Slope
- ● - ● - ● - ERF of A Theoretical Data Set
- X - X - X - LSF derived by a 5 Point Fit
- Δ - Δ - Δ - LSF derived by a 7 Point Fit
Optimum Edge Position
FWHM
'Step Effect'
Contrast Value
Pixel

Fig. 3

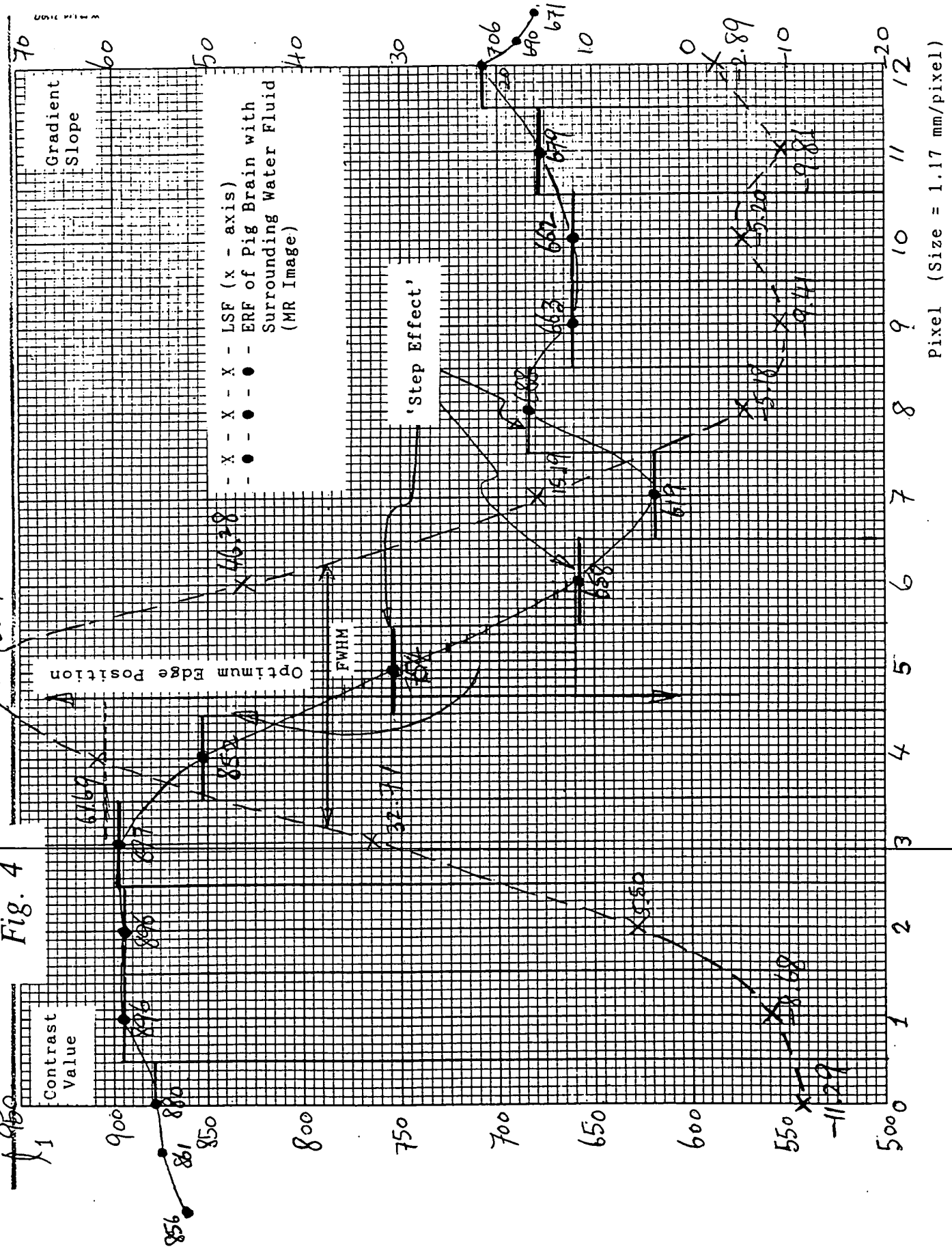
Gradient Slope
- X - X - X - LSF (x - axis)
- ● - ● - ● - ERF of Pig Brain with Surrounding Water Fluid (MR Image)
'Step Effect'
Optimum Edge Position
FWHM
Contrast Value
Pixel (Size = 1.17 mm/pixel)

Fig. 4

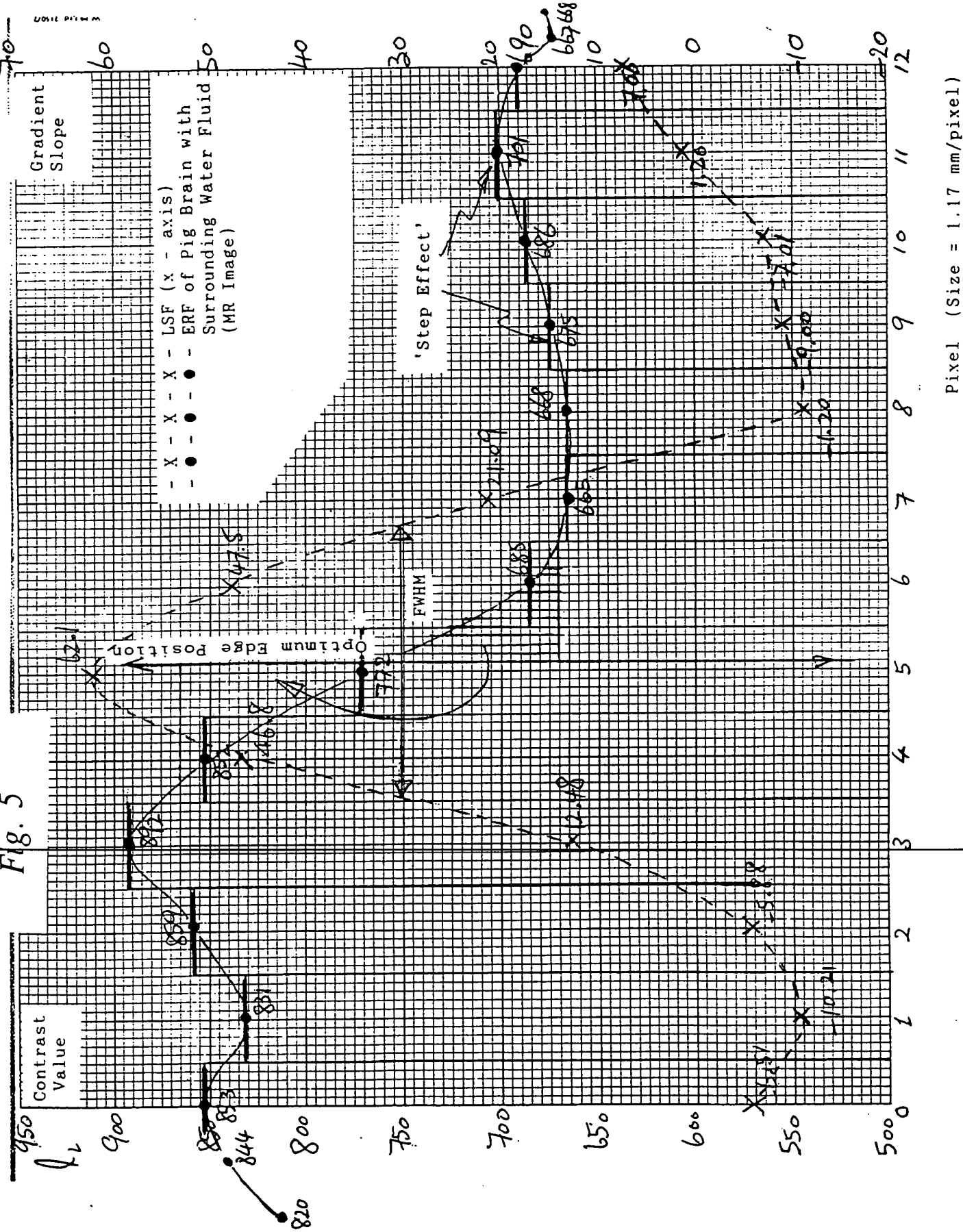
Gradient Slope
- X - X - X - LSF (x - axis)
- ● - ● - ● - ERF of Pig Brain with Surrounding Water Fluid (MR Image)
'Step Effect'
FWHM
Optimum Edge Position
Contrast Value
Pixel (Size = 1.17 mm/pixel)

Fig. 5

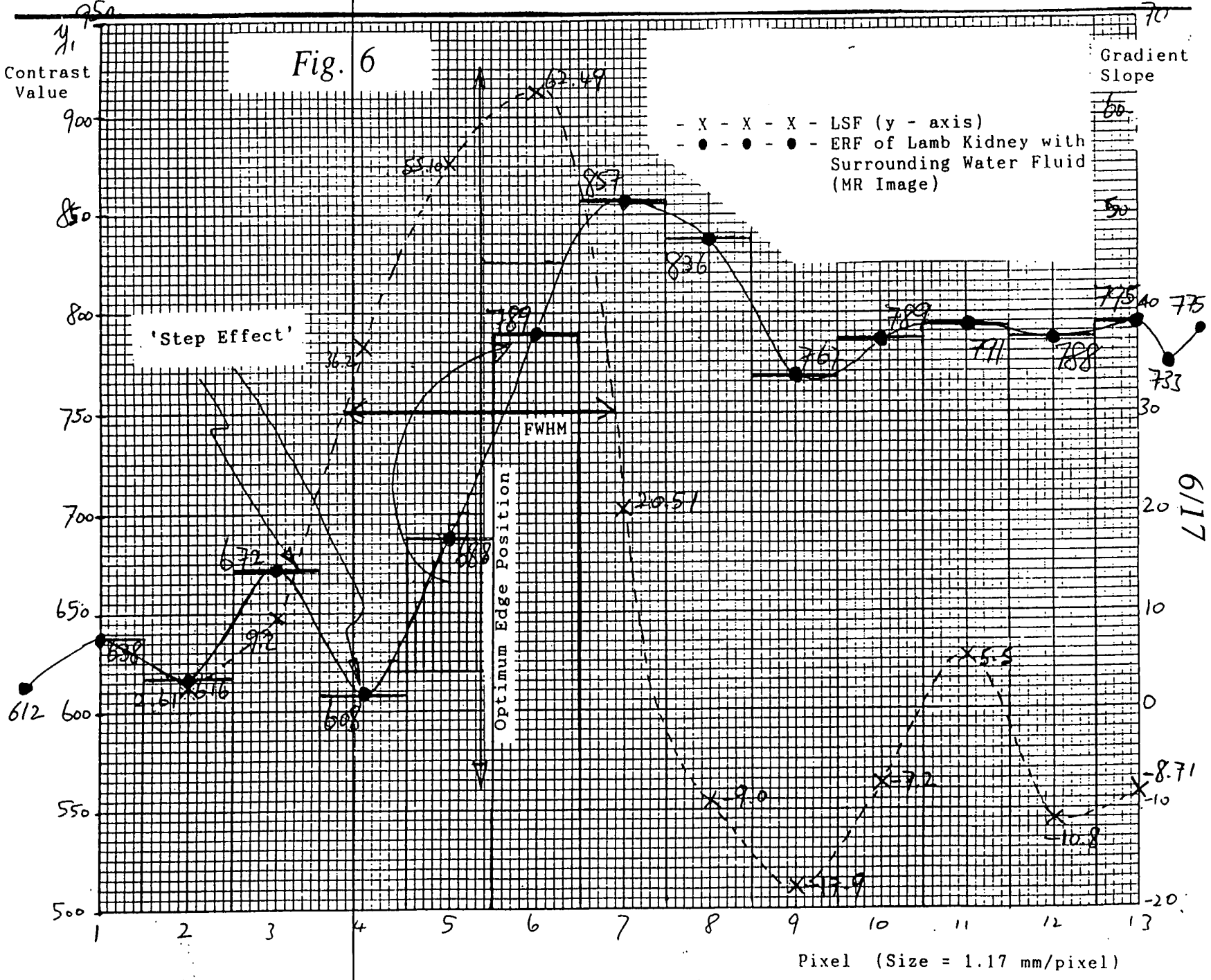
Fig. 6
Contrast Value
Gradient Slope
- X - X - X - LSF (y - axis)
- ● - ● - ● - ERF of Lamb Kidney with Surrounding Water Fluid (MR Image)
'Step Effect'
FWHM
Optimum Edge Position
Pixel (Size = 1.17 mm/pixel)

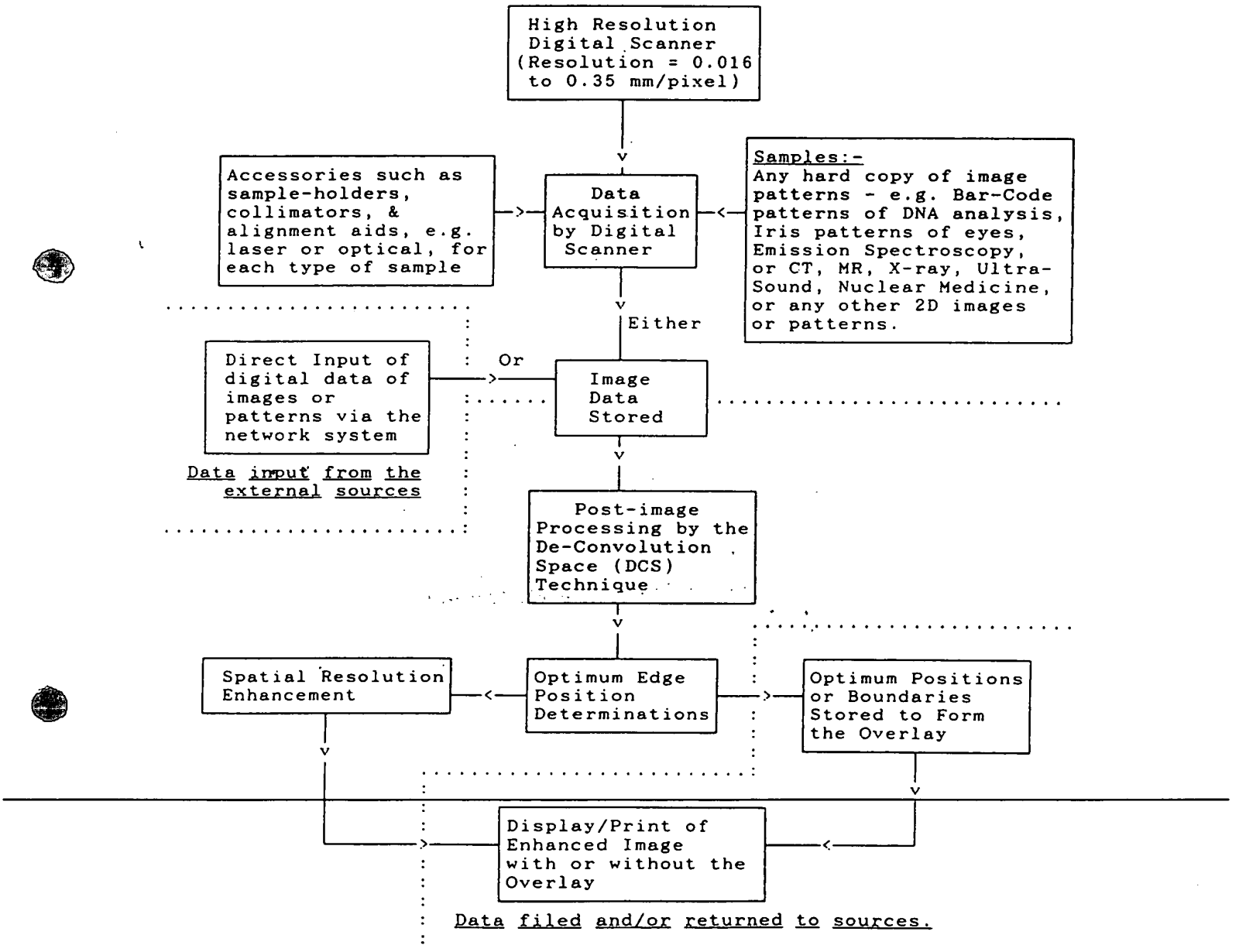
High Resolution Digital Scanner (Resolution = 0.016 to 0.35 mm/pixel)
Accessories such as sample-holders, collimators, & alignment aids, e.g. laser or optical, for each type of sample
Data Acquisition by Digital Scanner
Samples:-
Any hard copy of image patterns - e.g. Bar-Code patterns of DNA analysis, Iris patterns of eyes, Emission Spectroscopy, or CT, MR, X-ray, Ultra-Sound, Nuclear Medicine, or any other 2D images or patterns.
Either
Or
Direct Input of digital data of images or patterns via the network system
Image Data Stored
Data input from the external sources
Post-image Processing by the De-Convolution Space (DCS) Technique
Spatial Resolution Enhancement
Optimum Edge Position Determinations
Optimum Positions or Boundaries Stored to Form the Overlay
Display/Print of Enhanced Image with or without the Overlay
Data filed and/or returned to sources.

Fig. 7

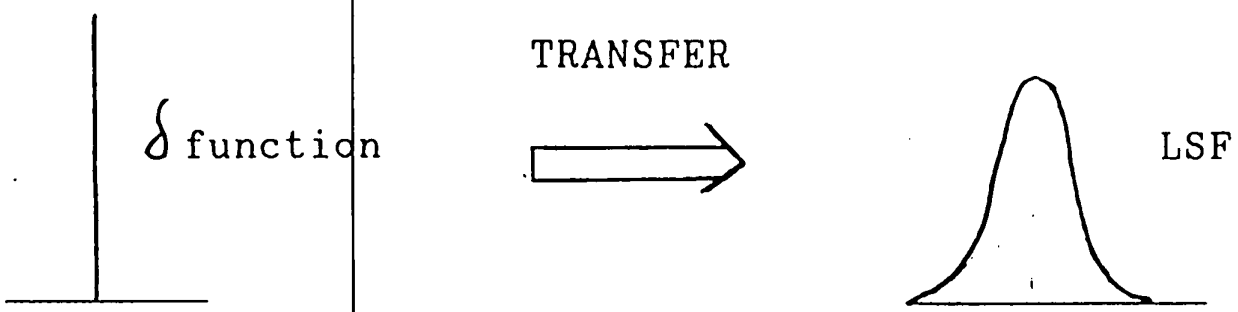
Object Domain
Image Domain
δ function
TRANSFER
LSF

Fig. 8

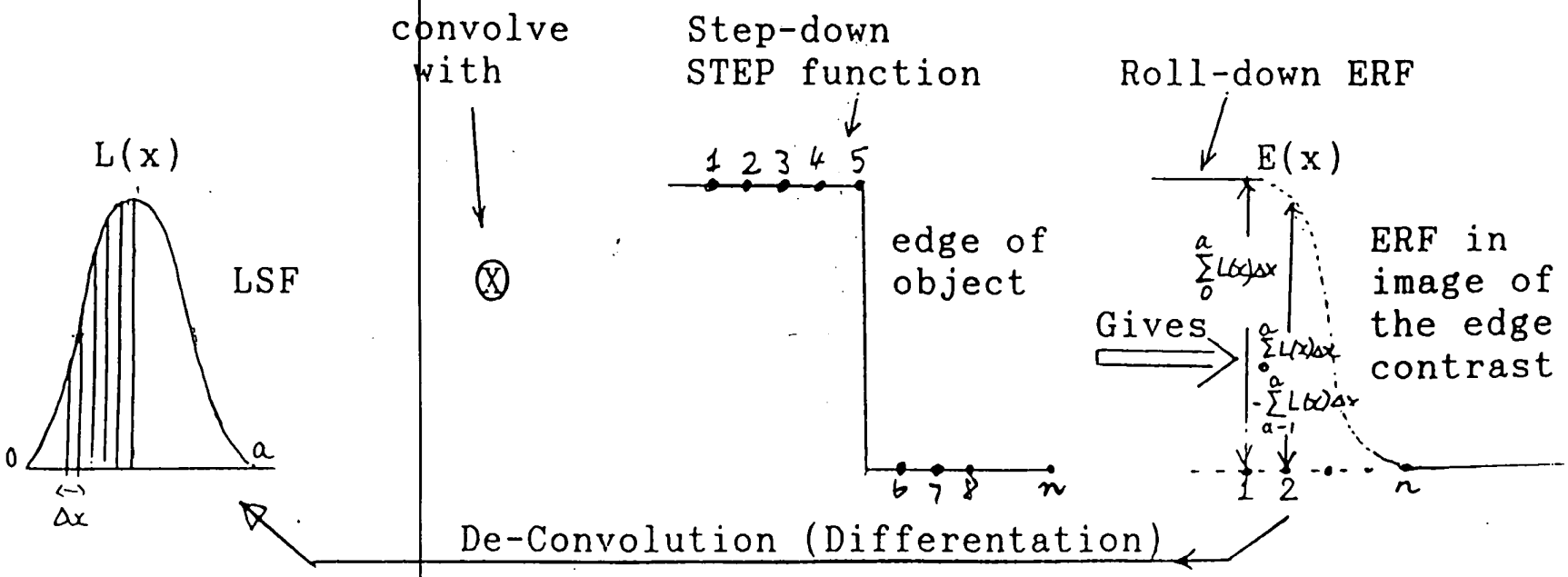
convolve with
Step-down STEP function
Roll-down ERF
L(x)
LSF
0
a
Δx
1 2 3 4 5
edge of object
E(x)
ERF in image of the edge contrast
Gives
1 2
n
De-Convolution (Differentation)

Fig. 9

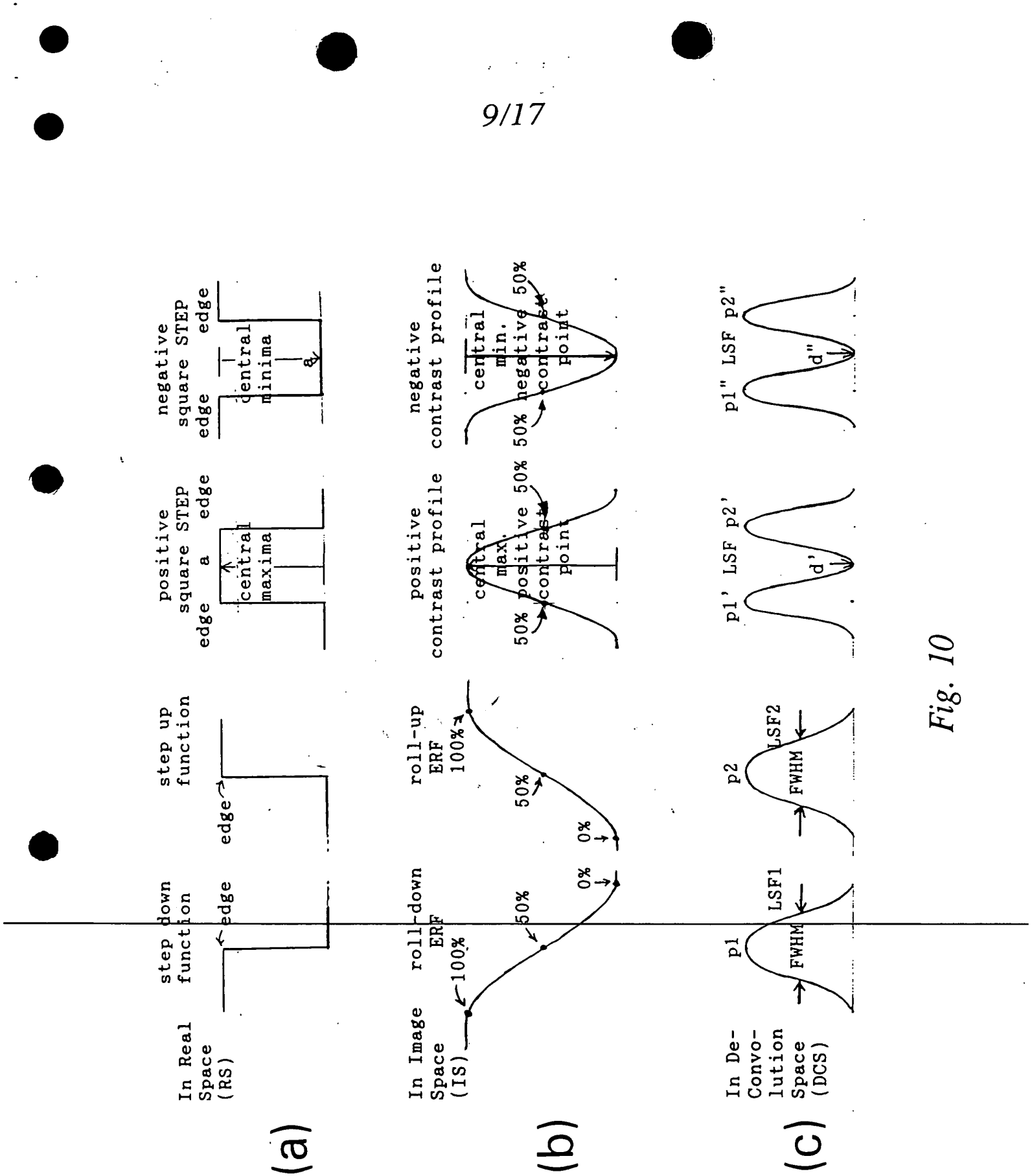
(a)
In Real Space (RS)
step down function
edge
step up function
edge
positive square STEP
edge a edge
central maxima
negative square STEP
edge edge
central minima
a
(b)
In Image Space (IS)
roll-down ERF
100%
50%
0%
roll-up ERF
100%
50%
0%
positive contrast profile
central max.
50% positive contrast point
negative contrast profile
central min.
50% negative contrast point
(c)
In De-Convo-lution Space (DCS)
p1
FWHM
LSF1
p2
LSF2
FWHM
p1' LSF p2'
d'
p1" LSF p2"
d"

Fig. 10

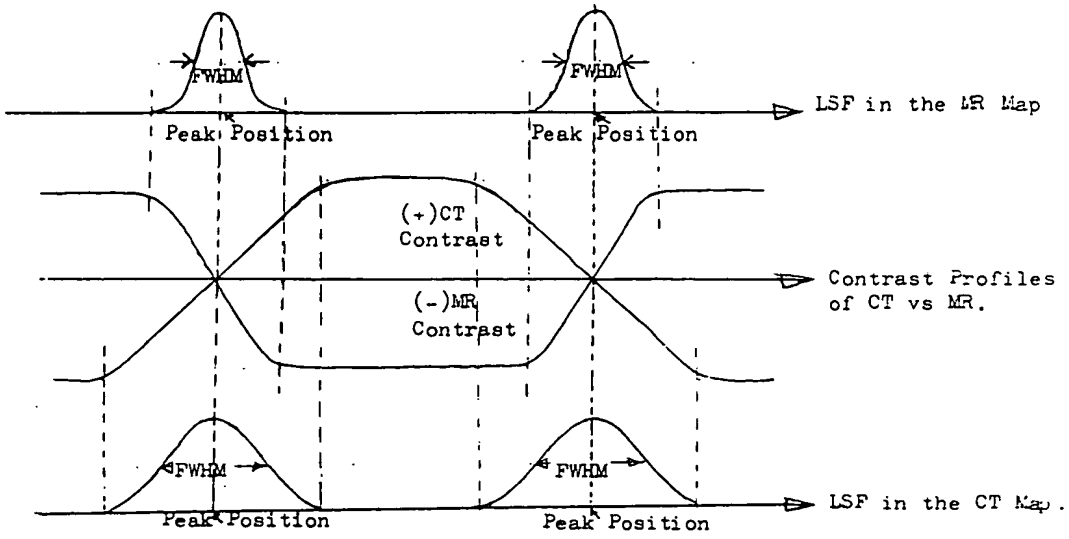
FWHM
FWHM
LSF in the MR Map
Peak Position
Peak Position
(+)CT
Contrast
(-)MR
Contrast
Contrast Profiles
of CT vs MR.
FWHM
FWHM
LSF in the CT Map.
Peak Position
Peak Position

Fig. 11

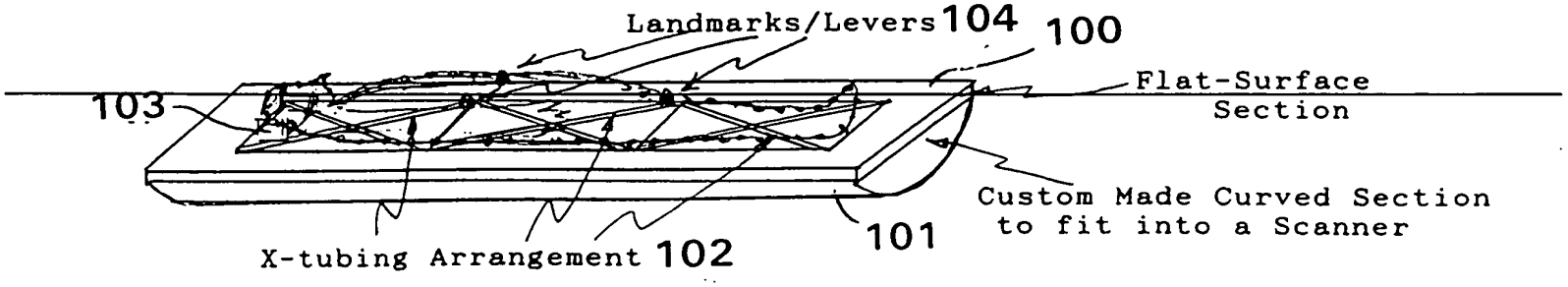
Landmarks/Levers 104
100
Flat-Surface
Section
103
Custom Made Curved Section
to fit into a Scanner
101
X-tubing Arrangement 102

Fig. 13

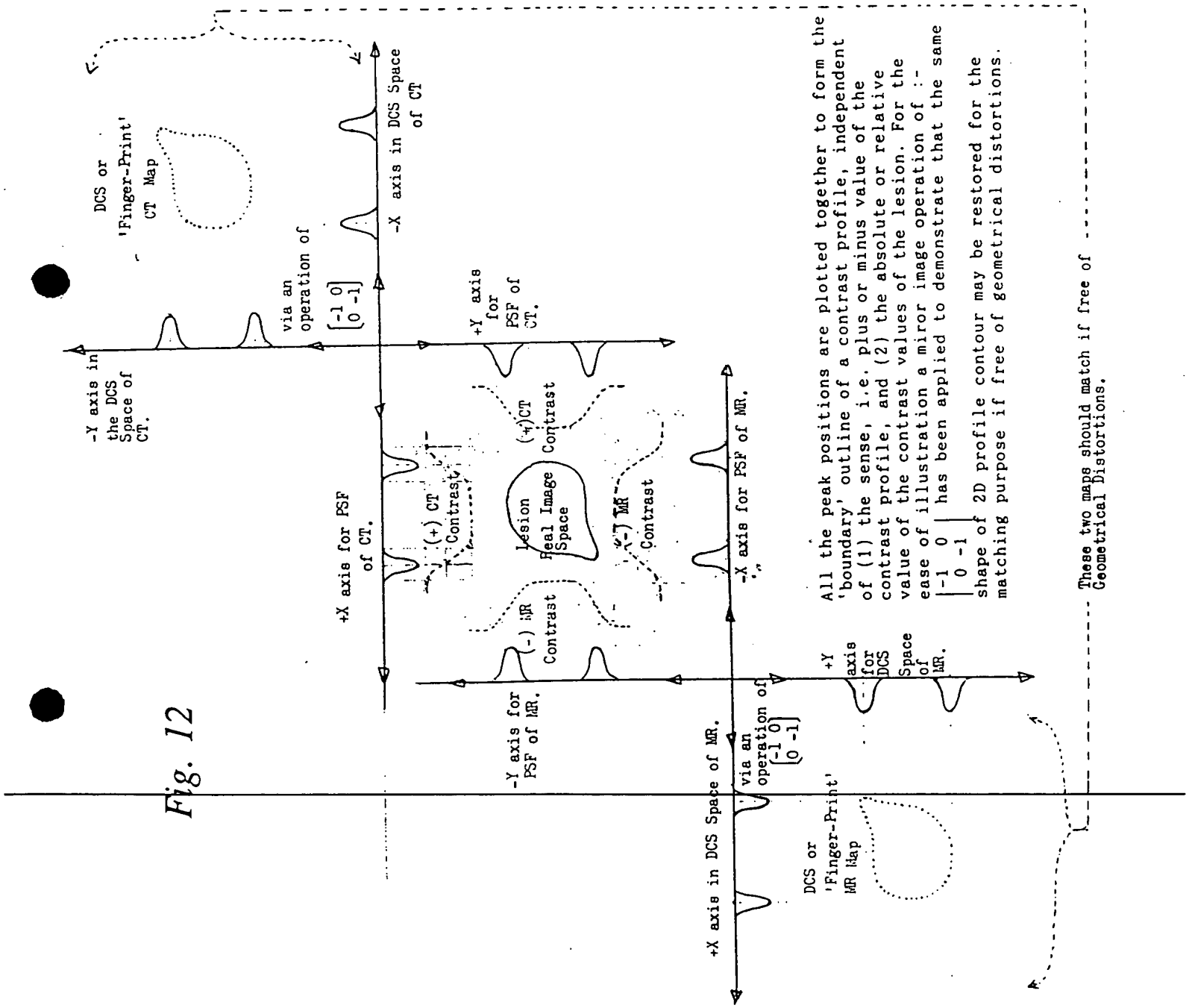
DCS or 'Finger-Print' CT Map
-Y axis in the DCS Space of CT.
via an operation of [-1 0 / 0 -1]
-X axis in DCS Space of CT
+Y axis for PSF of CT.
+X axis for PSF of CT.
(+) CT Contrast
(+) CT Contrast
Lesion Real Image Space
(-) MR Contrast
(-) MR Contrast
-X axis for PSF of MR.
-Y axis for PSF of MR.
+Y axis for DCS Space of MR.
via an operation of [-1 0 / 0 -1]
+X axis in DCS Space of MR.
DCS or 'Finger-Print' MR Map
All the peak positions are plotted together to form the 'boundary' outline of a contrast profile, independent of (1) the sense, i.e. plus or minus value of the contrast profile, and (2) the absolute or relative value of the contrast values of the lesion. For the ease of illustration a miror image operation of :- | -1 0 / 0 -1 | has been applied to demonstrate that the same shape of 2D profile contour may be restored for the matching purpose if free of geometrical distortions.
These two maps should match if free of Geometrical Distortions.

Fig. 12

Fig. 14

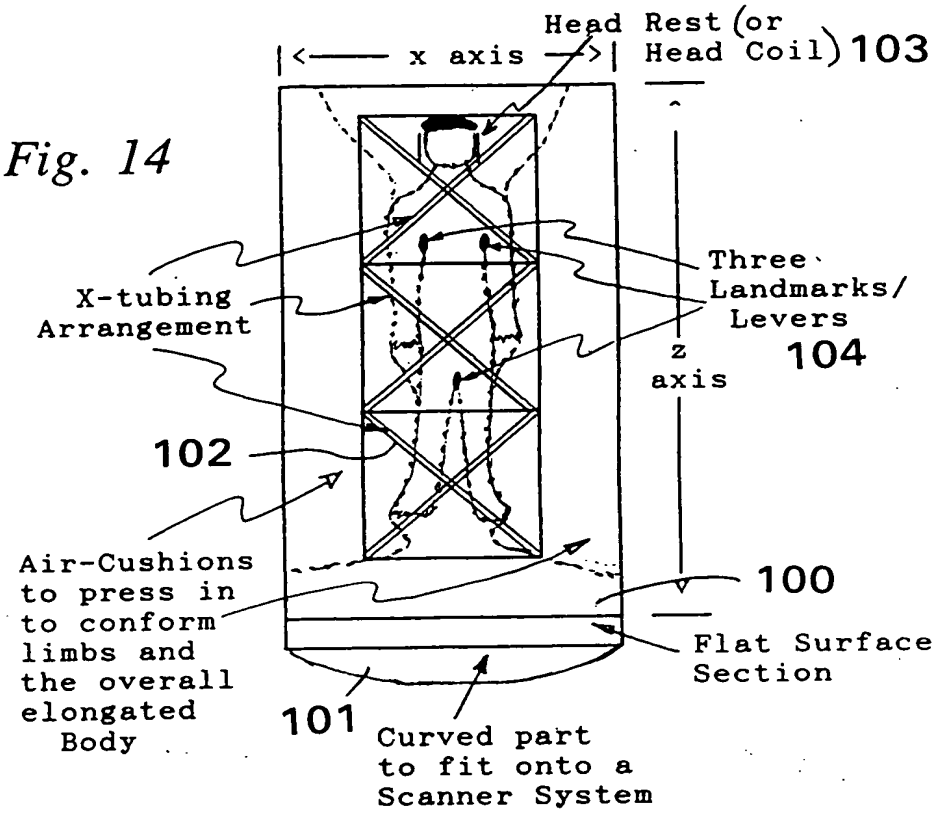
Head Rest (or Head Coil) 103
x axis
Three Landmarks/ Levers 104
z axis
X-tubing Arrangement
102
Air-Cushions to press in to conform limbs and the overall elongated Body
100
Flat Surface Section
101
Curved part to fit onto a Scanner System

Fig. 15

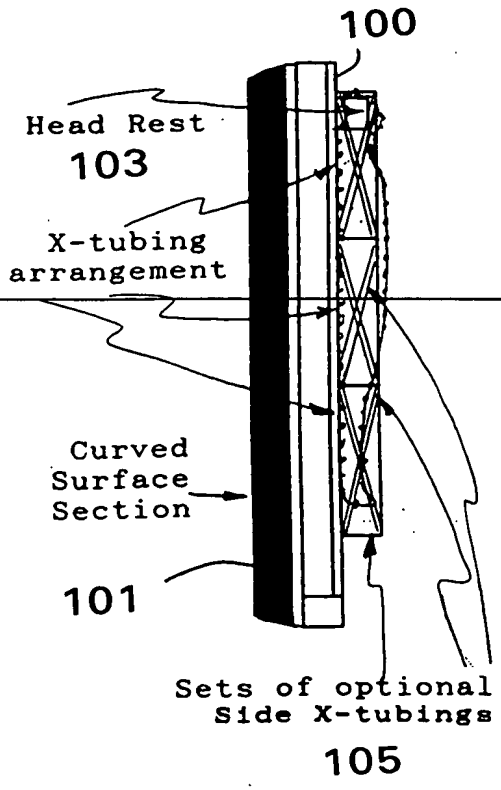
100
Head Rest 103
X-tubing arrangement
Curved Surface Section
101
Sets of optional Side X-tubings
105

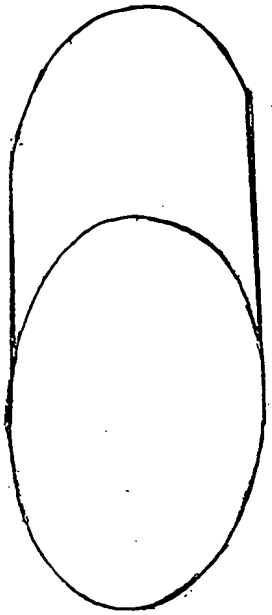

Fig. 18

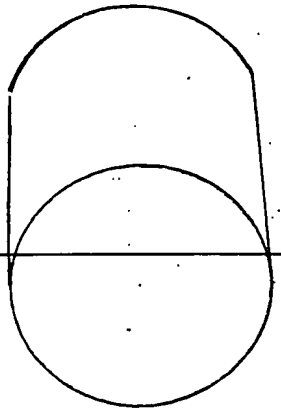

Fig. 16

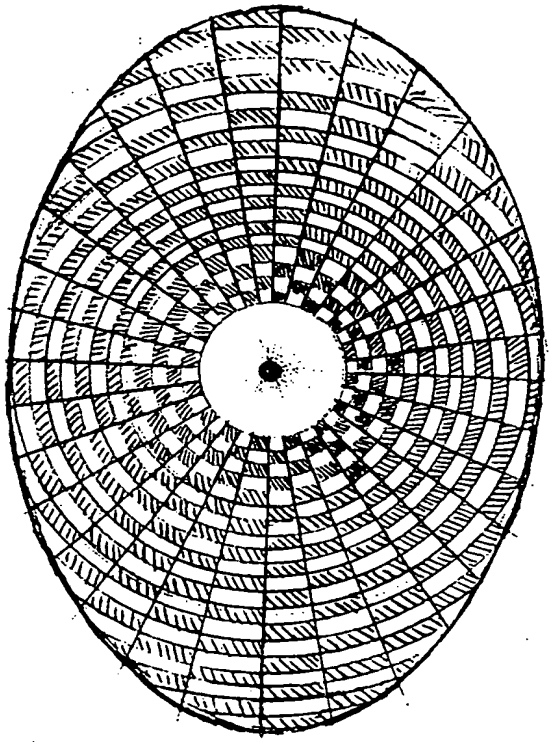

Fig. 19

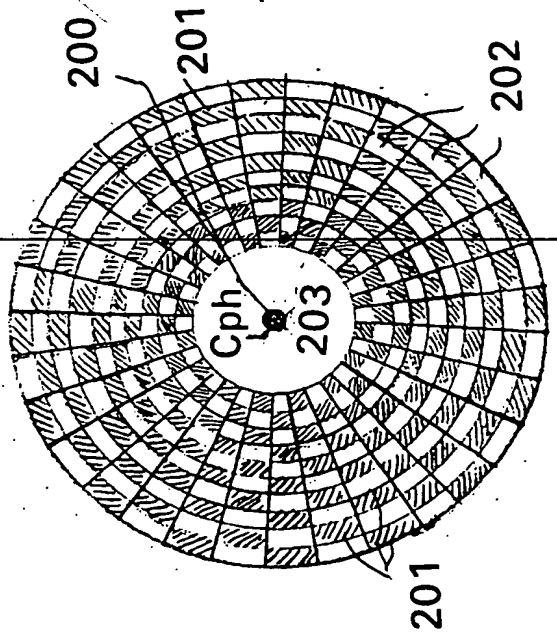

Fig. 17

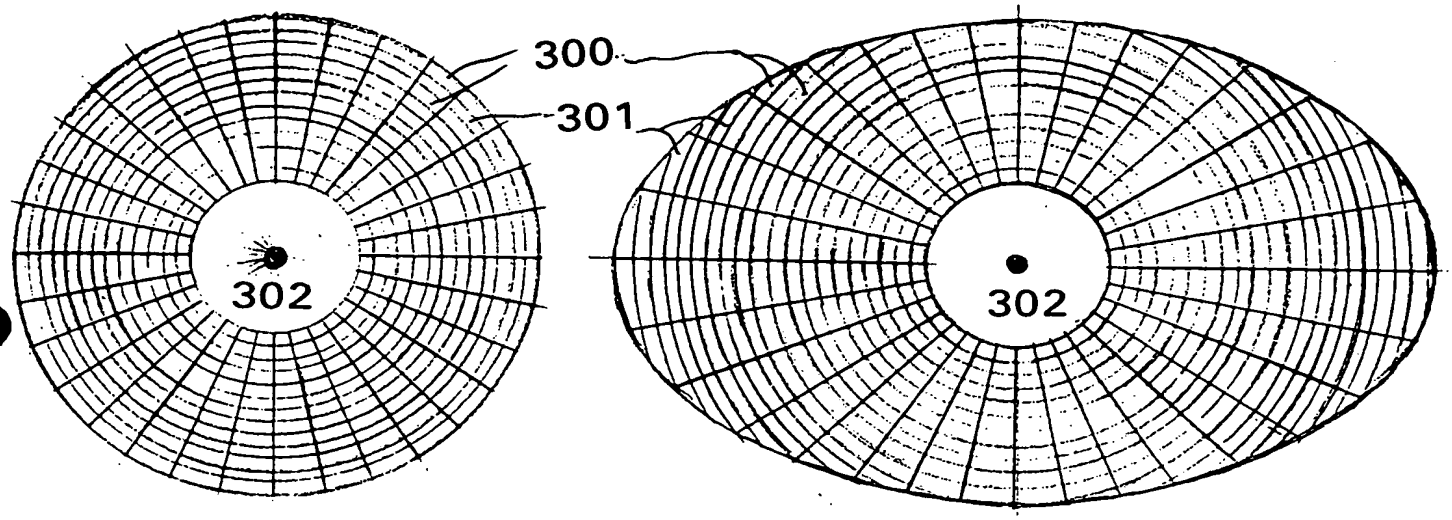

Fig. 20

Fig. 21

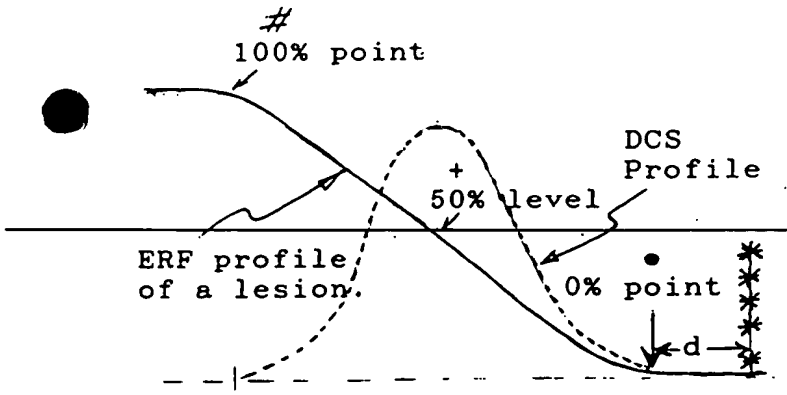

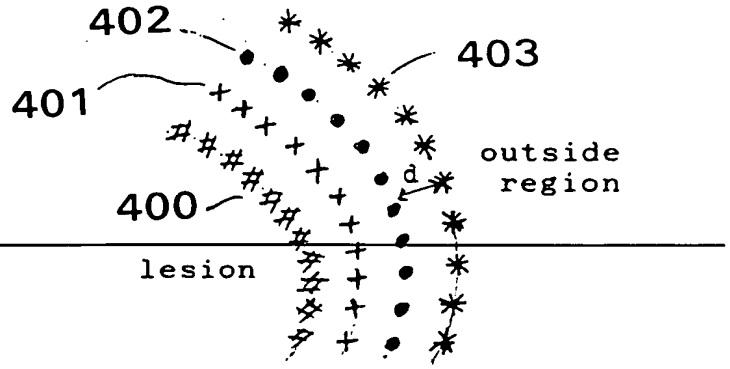

Fig. 22

Fig. 23

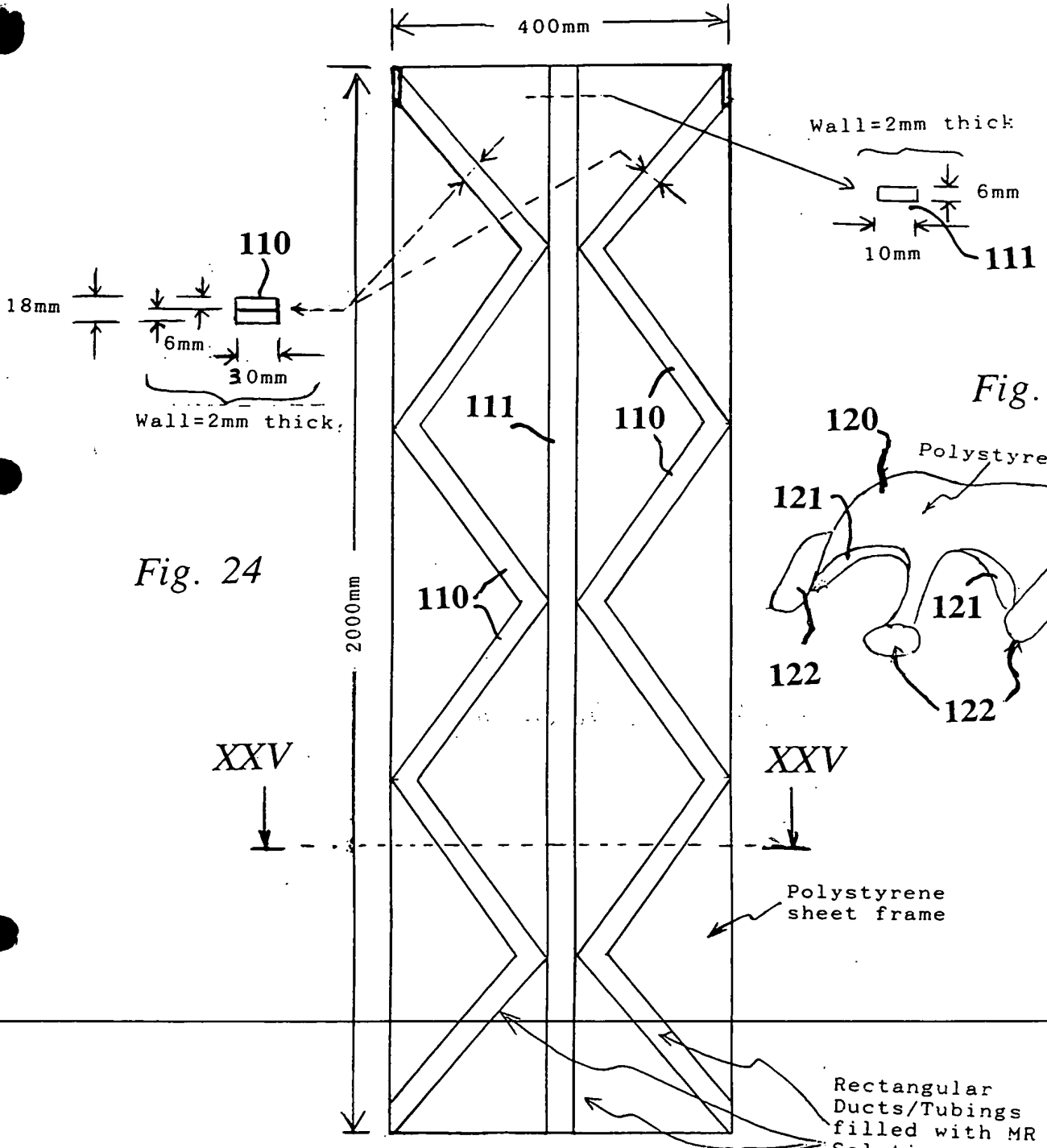

Fig. 24

Fig. 27

Fig. 25

Fig. 26

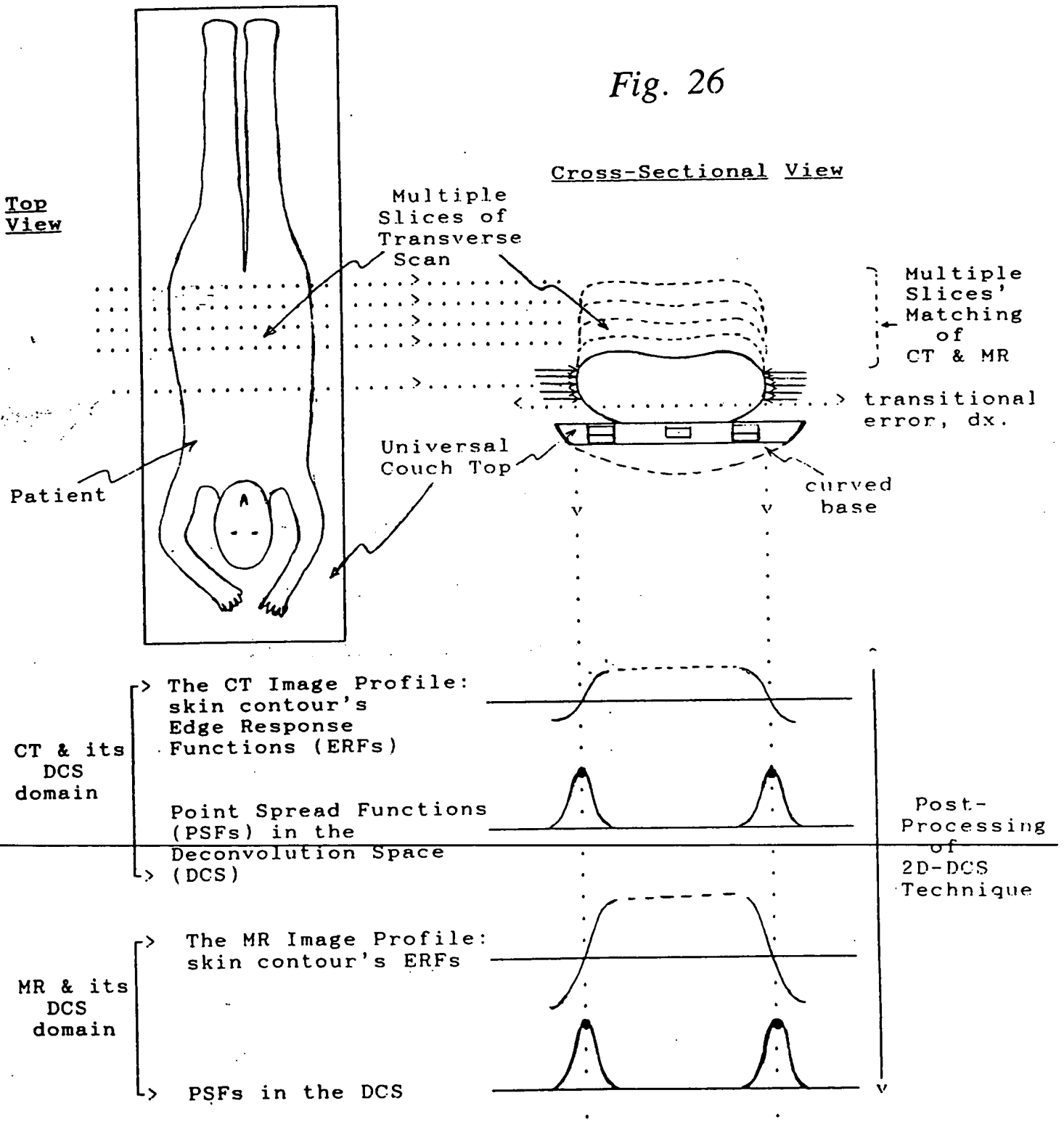
Top View
Cross-Sectional View
Multiple Slices of Transverse Scan
Multiple Slices' Matching of CT & MR
transitional error, dx.
Universal Couch Top
Patient
curved base
CT & its DCS domain
The CT Image Profile: skin contour's Edge Response Functions (ERFs)
Point Spread Functions (PSFs) in the Deconvolution Space (DCS)
Post-Processing of 2D-DCS Technique
MR & its DCS domain
The MR Image Profile: skin contour's ERFs
PSFs in the DCS

The Overall Flow-chart

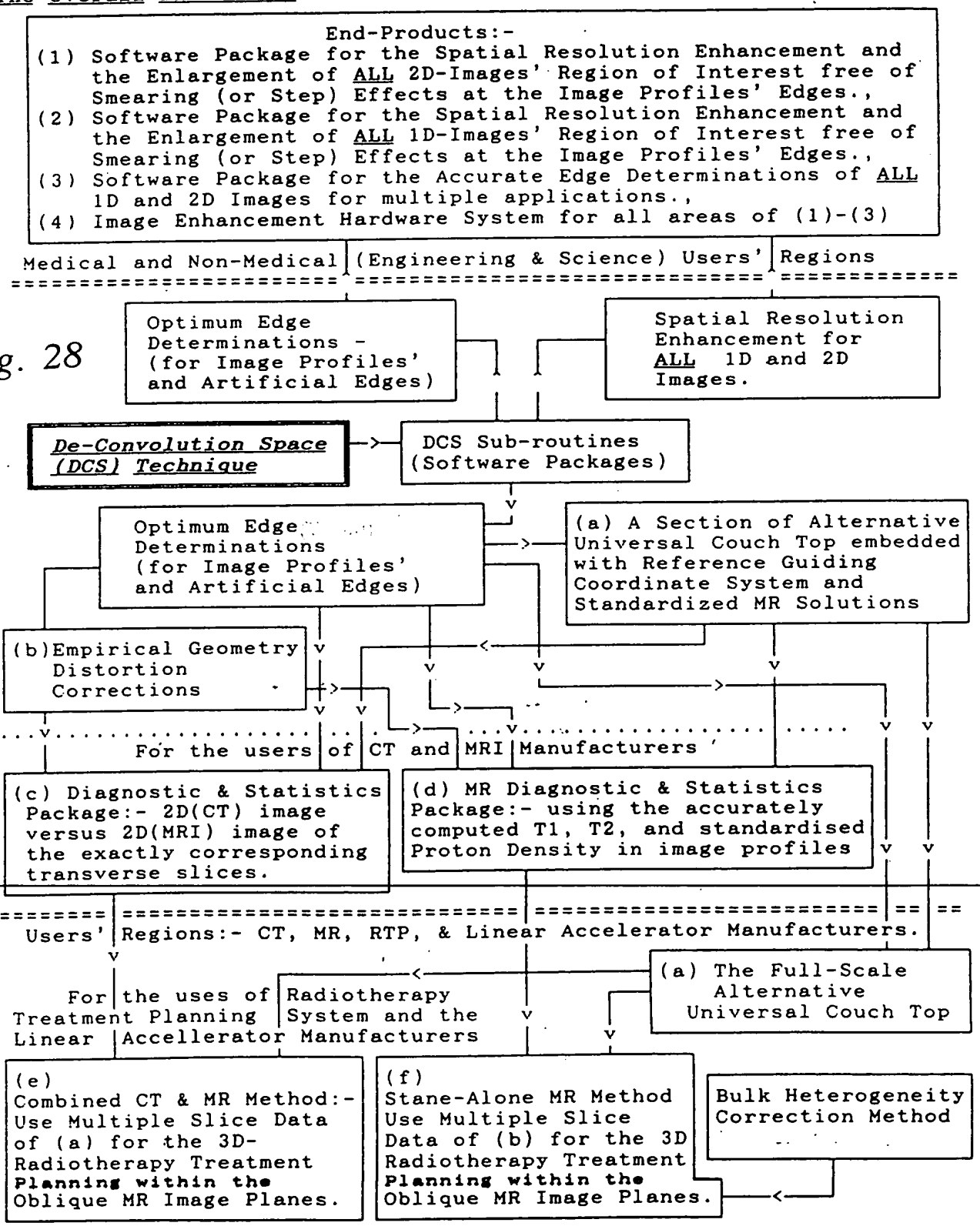

Fig. 28

PCT/GB99/03417

Graham Coles & Co.

8.11.99